

A Universal Framework for Large-Scale Multi-Objective Optimization Based on Particle Drift and Diffusion

Jia-Cheng Li, Min-Rong Chen, Guo-Qiang Zeng, Jian Weng, Man Wang, Jia-Lin Mai, *Member, IEEE*

Abstract—Large-scale multi-objective optimization poses challenges to existing evolutionary algorithms in maintaining the performances of convergence and diversity because of high dimensional decision variables. Inspired by the motion of particles in physics, we propose a universal framework for large-scale multi-objective optimization based on particle drift and diffusion to solve these challenges in this paper. This framework innovatively divides the optimization process into three sub-stages: two coarse-tuning sub-stages and one fine-tuning sub-stage. Different strategies of drift-diffusion operations are performed on the guiding solutions according to the current sub-stage, ingeniously simulating the movement of particles under diverse environmental conditions. Finally, representative evolutionary algorithms are embedded into the proposed framework, and their effectiveness are evaluated through comparative experiments on various large-scale multi-objective problems with 1000 to 5000 decision variables. Moreover, comparative algorithms are conducted on neural network training problems to validate the effectiveness of the proposed framework in the practical problems. The experimental results demonstrate that the framework proposed in this paper significantly enhances the performance of convergence and diversity of MOEAs, and improves the computational efficiency of algorithms in solving large-scale multi-objective optimization problems.

Index Terms—Large-scale multi-objective optimization, evolutionary algorithms, drift-diffusion operations.

I. INTRODUCTION

THE characteristic of multi-objective optimization problems (MOPs) is the need to simultaneously optimize a set of typically conflicting objective functions [1]–[4]. This conflict results in the absence of a unique global optimal solution for MOPs, and only a set of trade-off solutions between objectives can be obtained. To address Multi-Objective Problems (MOPs), a number of traditional multi-objective evolutionary algorithms (MOEAs) have been proposed. These include: NSGA-II [5], which employs fast non-dominated sorting and crowding distance; NSGA-III [6], built upon a set of reference vectors; MOEA/D [7], based on problem decomposition; and C-TAEA [8], which utilizes a dual-archive mechanism to maintain high-quality solutions. Large-scale multi-objective optimization problems (LSMOPs), characterized by hundreds or thousands of decision variables, have become increasingly prevalent in real-world engineering design in recent years, such as power system optimization [9], traffic scheduling [10], machine learning [11], network design optimization [12]. As the dimensionality of decision variables increases, finding effective solutions within these high-dimensional decision spaces becomes exponentially more

challenging. Traditional MOEAs generally overlook the scalability of decision variables within MOPs, which undermines the performance in solving LSMOPs. Therefore, the challenge lies in designing specialized MOEAs that enhance search efficiency while strictly controlling function evaluations (FEs).

According to the characteristics of existing metaheuristic MOEAs for solving LSMOPs, they can be broadly categorized into three main categories. The first widely adopted approach is decision variable decomposition by using the divide-and-conquer mechanism, such as cooperative coevolution (CC) employing random grouping [13]–[15], differential grouping [16], [17], or other grouping techniques [18]–[21]. The second category focuses on designing novel and powerful search operators or variation methods [22]–[27], such as introducing specialized genetic operators and competitive learning strategies. Based on transforming the problem [28]–[30], the third approach involves creating a reduced-scale version of the original problem for optimization in a less complex space.

Although these MOEAs have shown promise in solving LSMOPs, there is increasingly interest in developing comprehensive frameworks. These frameworks provide a modular structure that can embed different MOEAs to solve LSMOPs, thereby fully utilizing the advantages of various algorithms. Considering these significant advantages, several representative frameworks have been proposed to solve LSMOPs. Zille et al. [28] proposed a weight optimization framework (WOF for short), which transforms large-scale problems into smaller-scale weight optimization problems by variable grouping and assigns each group of variables to a weight variable. However, WOF has certain limitations [31]. On the one hand, WOF is restricted by the chosen variable grouping technique; On the other hand, WOF cannot fine-grained tune variables since these variables are assigned to the same weight variables, limiting the coverage of the search space. To enhance the coverage of the search space, He et al. [29] proposed a problem reconstruction framework (LSMOF for short) using bi-directional search directions, which reformulates the LSMOP into a single-objective problem with weight variables. A notable improvement in LSMOF over WOF is the introduction of weight variables tied to two search directions. However, a significant limitation stems from its reliance on the specific direction vectors employed [31], [32]. Additionally, the transformation function may cause information loss, affecting the quality of the final solution. The fuzzy decision variable framework (FDV) was proposed by Yang et al. [33]. This framework applies fuzzification to decision variables, with the degree of

fuzzification gradually decreasing as the evolutionary process progresses. However, the parameters *Rate* and *Acc* in FDV have a significant impact on the results and need to be properly adjusted for different problems to ensure the effectiveness of algorithms [34].

Inspired by the motion of particles in physics, we propose a novel optimization framework based on particle drift and diffusion (PDD for short) to solve LSMOPs. In contrast to traditional heuristic algorithms that use the singular strategy, our framework presents distinct advantages stemming from its flexible multi-stage particle guidance mechanism. The main contributions of this work are summarized as follows:

- 1) A guiding particle selection strategy is proposed to identify a set of high-quality particles from the population that helps to enhance the performance of convergence and diversity. These high-quality particles are referred as guiding particles in this paper. To effectively select the guiding particles, an improved angle penalty distance calculation method (IAPD for short) is proposed.
- 2) A sub-stage division method is presented to divide the entire optimization process into three sub-stages: two coarse-tuning sub-stages and a fine-tuning sub-stage. This method can adaptively adjust different strategies of drift-diffusion operations according to the current sub-stage.
- 3) A particle drift-diffusion process is proposed. During the coarse-tuning sub-stage, both drift and diffusion operations are performed to simulate the motion patterns of particles. During the fine-tuning sub-stage, only diffusion operation is performed to conduct refined local search around the guiding particles.
- 4) A gradual shrinking diffusion operator is put forward, which gradually reduces the diffusion range of particles for generating new solutions as the optimization advances. This method allows for comprehensive exploration of sub-regions surrounding the original solutions.

The remaining sections of this paper are organized as follows. In Section II, we review several relevant theoretical knowledge used to propose the PDD framework. In Section III, a detailed description of the PDD framework and the main procedure of the proposed algorithm are presented. The experimental settings and the analysis on experimental results are provided in Section IV. Finally, the conclusion and future works are drawn in Section V.

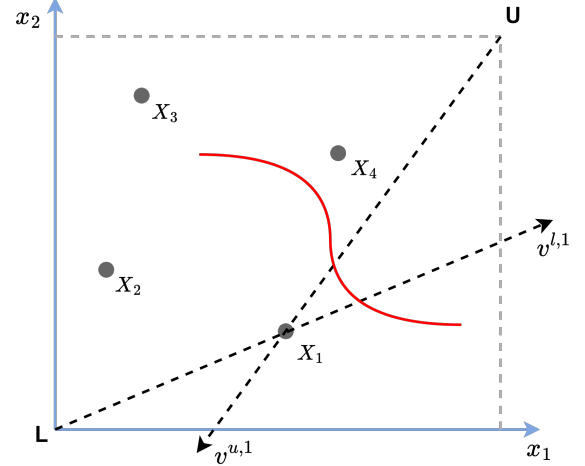
II. PRELIMINARIES AND MOTIVATION

In this section, we first recall the related work on large-scale multi-objective optimization. Then, the motivations of designing a new large-scale MOEA framework are given.

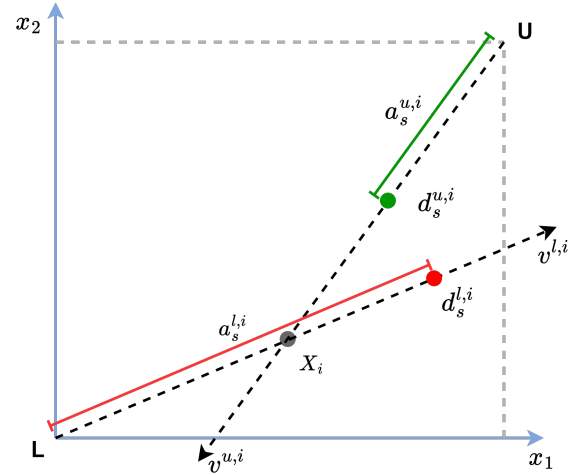
A. Multi-Objective Optimization Problems

MOPs involve multiple conflicting objectives that are typically mutually contradictory, where optimizing one objective may lead to the degradation of others. MOPs can be mathematically defined as the following [35]:

$$\begin{aligned} & \text{minimize } F(X) = (f_1(X), f_2(X), \dots, f_M(X)) \\ & \text{subject to } X \in \Omega \end{aligned} \quad (1)$$



(a)



(b)

Fig. 1. (a) Two search directions are defined based on selected solutions, lower and upper bound solutions in the decision space. (b) An illustration depicts random sampling along two search directions based on selected solutions.

where $X = (x_1, x_2, \dots, x_D)$ is an D -dimensional decision variable vector in the decision space Ω , and M is the number of objectives. $F(X)$ is the objective function vector consisting of M mutually conflicting objective functions. Due to the conflicting nature of the objectives in MOPs, there is usually no single solution that can simultaneously optimize all objectives. Instead, a set of trade-off solutions is usually obtained to approach the Pareto front (PF).

B. Angle-Penalized Distance

For the purpose of achieving a balance between diversity and convergence in MOEAs, Cheng et al. [29] proposed a scalarization approach called angle-penalized distance (APD). APD is defined as the following Eqs. (2-5):

$$d_{i,j} = (1 + P(\theta_{i,j})) \cdot \|f'_i\| \quad (2)$$

$$P(\theta_{i,j}) = M \cdot (R_{FE})^\alpha \cdot \frac{\theta_{i,j}}{\gamma_{w_j}} \quad (3)$$

$$\gamma_{w_j} = \min_{i \in \{1, \dots, N_w\}, i \neq j} \{w_i, w_j\} \quad (4)$$

$$f'_i = f_i - z_i^{min} \quad (5)$$

where M is the number of objectives, N_w is the number of reference vectors, $\theta_{i,j}$ is the angle between the i -th individual and the j -th reference vector w_j , and γ_{w_j} is the minimum angle between w_j and other reference vectors. f_i and f'_i denote the original and translated objective vectors of the i -th individual, respectively. $z^{min} = (z_1^{min}, z_2^{min}, \dots, z_M^{min})$ represents the minimum objective values used for translation, and $\|\cdot\|$ denotes the Euclidean norm. R_{FE} is the ratio of the current number of function evaluations ($FE_{current}$) to the maximum allowed (FE_{max}).

The core component of the APD, $d_{i,j}$, considers both the performance of convergence and diversity. The term $\|f'_i\|$ measures the distance of the translated objective vector f'_i to the ideal point, thus promoting the convergence. The penalty term $P(\theta_{i,j})$ encourages diversity by penalizing individuals based on their angular deviation from the reference vectors. In Eq. (3), the value of $(R_{FE})^\alpha$ increases as R_{FE} increases when α equals to 2, causing $P_{\theta_{i,j}} \approx 0$ in the early stage while gradually accumulating in the late stage. From Eq. (2), it can be observed that the intention of APD is to emphasize the convergence criterion $\|f'_i\|$ during the early search process. As the optimization process progresses, APD increasingly emphasizes the diversity criterion $\theta_{i,j}$ by accumulating the penalty term $P_{\theta_{i,j}}$. In this paper, we propose a modified version of APD, adapted for integration within our proposed PDD framework.

C. Application of Bidirectional Vectors

The integration of bidirectional vectors with search strategies has emerged as a promising research direction, because it can significantly increase the probability of intersection between the direction vector and the PF. Recent studies have particularly focused on incorporating bidirectional vectors into MOEAs to improve their performance of multi-objective optimization tasks. In the work of He et al. [29], the LSMOF integrates bidirectional vectors with sub-problem construction to improve global optimization by optimizing weight variables. Similarly, by introducing bidirectional vectors into LMOEA-DS, Qin et al. [30] proposed a method to randomly sample multiple solutions along the search direction and subsequently select non-dominated solutions among them.

Next, detailed descriptions of directional sampling based on bidirectional vectors in LMOEA-DS are provided. Firstly, solutions within the population are assigned to their closest reference vector, denoted as W . And then, one solution is selected for each reference vector based on the minimum projected distance, serving as a candidate solution. As shown in Fig. 1, for each candidate solution, two search directions are defined: $v^{l,1}$ and $v^{u,1}$, ..., $v^{l,i}$ and $v^{u,i}$, where i ranges from 1 to N_w , where N_w represents the number of reference vectors.

The search directions $v^{l,i}$ and $v^{u,i}$ originate from the lower bound point L and the upper bound point U , respectively. For example, in the two-dimensional decision space, the search direction of a solution $X_i = (x_{i,1}, \dots, x_{i,D})$ can be defined as follows:

$$\begin{aligned} v^{l,i} &= X_i - L \\ v^{u,i} &= X_i - U \end{aligned} \quad (6)$$

Assuming $d_j^{l,i}$ and $d_j^{u,i}$ are the solutions of randomly sampling along two search directions $v^{l,i}$ and $v^{u,i}$, respectively, which can be formulated as follows:

$$\begin{aligned} d_s^{l,i} &= L + a_s^{l,i} \cdot \frac{v^{l,i}}{\|v^{l,i}\|} \\ d_s^{u,i} &= U + a_s^{u,i} \cdot \frac{v^{u,i}}{\|v^{u,i}\|} \end{aligned} \quad (7)$$

where $a_s^{l,i}$ and $a_s^{u,i}$ are random numbers uniformly distributed in the interval $[0, \|U - L\|]$. The value of $a_s^{l,i}$ and $a_s^{u,i}$ determine the positions of the s -th sampling solution along the $v^{l,i}$ and $v^{u,i}$ directions, respectively. In this paper, we employ directed sampling operations to simulate drift motion. The parameter sampling frequency S is to control the number of sampled solutions generated along the two search directions $v^{l,i}$ and $v^{u,i}$.

D. The Motion of Particles

In the physical world, the motion of particles exhibits complex behaviors that are not only influenced by the intrinsic properties of particles but also by external environments and force fields. The diffusion motion is typically described as the random motion of free particles, which refers to the spontaneous movement of particles from high-concentration regions to low-concentration regions. As theories advanced, a substantial amount of research has been proposed from the perspective of diffusion motion, such as Markov process, harmonic functions, equilibrium measures, polar set and capacity analyses. These theories provide rich tools and perspectives for understanding the random diffusion behavior of particles. Particle motion can also be affected by external forces, resulting in drift. The drift refers to the directional movement of particles under the influence of external force fields, typically driven by environmental changes or external control parameters. In contrast to the diffusion process, the drift process is more directional, guiding particles towards potential optimal regions in optimization problems.

As far as we are aware, no existing literature has explored the application of particle motion principles in LSMOPs. Simulating and harnessing the characteristics of particle motion may offer a novel pathway to derive effective solutions for LSMOPs.

E. Motivation

The performance of existing large-scale MOEAs in solving LSMOPs is unsatisfactory, because they struggle to simultaneously maintain an adequate balance between convergence and diversity. On the one hand, MOEAs need to thoroughly explore the vast search space in order to enhance convergence.

Algorithm 1 Main Framework of the Proposed PDD

Input: N (the population size), FE_{max} (the maximum value of function evaluations), $Rate$ (the coarse-tuning ratio)

Output: P (the population)

- 1: $P = Initialization(N)$
- 2: $RefV = UniformReferencePoint(N)$
- 3: $CSL = Sub-stage_Division(Rate)$
- 4: **while** $FE_{current} < FE_{max}$ **do**
- 5: $P' = Operator(P)$
- 6: $R_{FE} = FE_{current}/FE_{max}$
- 7: $Prob = \min((R_{FE}/3 - 1)^2, Up)$
- 8: **if** $rand < Prob$ **then**
- 9: $Q = PDD_Process(P, RefV, CSL, Rate)$
- 10: $P' = P' \cup Q$
- 11: **end if**
- 12: $P = Environmental_Selection(P \cup P')$
- 13: **end while**
- 14: **return** P

However, this makes it challenging to find a sufficient number of different solutions within a limited number of iterations, resulting in the generated solution cannot fully cover the entire PF. On the other hand, excessive emphasis on diversity can impede the convergence efficiency of populations towards the PF. Furthermore, the inherent complexity of high-dimensional search spaces exacerbates the difficulty in balancing convergence and diversity, as MOEAs become more susceptible to premature convergence to local optima within these high-dimensional decision spaces.

In the physical world, numerous instances of particle diffusion can be observed, such as in gases, liquids, and heat transfer phenomena. These exemplify an inherent stochastic motion. Additionally, particles may undergo directed drift under the influence of external forces. Inspired by these fundamental physical processes, we propose a novel framework for solving LSMOPs, which simulates both particle drift and diffusion. Unlike conventional MOEAs, this dual-mechanism approach capitalizes on the distinct characteristics of drift and diffusion, which enables extensive exploration and refined search.

The drift motion along specific directions allows particles to rapidly converge towards potential optimal regions, thereby enhancing the global search efficiency of algorithms. Meanwhile, this directional movement empowers particles to escape from local optima, mitigating the risk of premature convergence. Conversely, the disordered diffusion motion enables an exhaustive exploration of local sub-regions, strengthening the local search capabilities of algorithm. As the particles approach the PF, diffusion facilitates fine-grained adjustments, refining the solution quality and ensuring a more precise approximation of the optimal set.

III. THE PROPOSED FRAMEWORK

The main structure of the proposed framework based on particle drift and diffusion is outlined in Algorithm 1. First, The population P and a reference point set $RefV$ are initialized. The *Sub-stage_Division* function divides the entire op-

Algorithm 2 Particle Drift-Diffusion Process

Input: N (the population size), P (the population), $RefV$ (a set of reference vectors), $Rate$ (the coarse-tuning ratio), CSL (sub-stage cumulative step length)

Output: Q (a set of solutions)

- 1: $N_{w'} = \lceil N/10 \rceil$
- 2: $X_1^* = \emptyset, X_2^* = \emptyset$
- 3: $X = Guiding_Particle_Selection(P, RefV, N_{w'})$
- 4: **for** $k = 1 : 3$ **do**
- 5: **if** $R_{FE} \geq CSL(k-1)$ **and** $R_{FE} < CSL(k)$ **then**
- 6: Generate diffusion particles X_1^* for X using Eq. (11);
- 7: **if** $R_{FE} < Rate$ **then**
- 8: Generate drifting particles X_d for X using Eq. (6-7);
- 9: Generate diffusion particles X_2^* for X_d using Eqs. (11);
- 10: **end if**
- 11: **end for**
- 12: **end for**
- 13: $Q = X_1^* \cup X_2^*$
- 14: **return** Q

timization process into three sub-stages: two fuzzy sub-stages and a precise optimization sub-stage. It returns the cumulative step length of sub-stages, denoted as CSL (line 3). Then, the offspring P' is generated using the offspring generation method of the embedded MOEA (line 5). For example, if the embedded MOEA is NSGAI, then the offspring generation method uses crossover and mutation operations to create a new population. R_{FE} represents the ratio of the $FE_{current}$ to the FE_{max} , increasing from 0 to 1 as the optimization advances (line 6). If the random number $rand$ is less than $Prob$, which indicates the probability of triggering the *PDD_Process*, the *PDD_Process* function is invoked to generate additional offspring solutions Q , which are then added to the offspring collection (lines 8-11). Finally, the next-generation population is then evaluated by the MOEA embedded in the environment selection method (line 12). The detailed description is given in the subsequent subsections.

A. Particle Drift-Diffusion Process

Particles in physical systems inherently exhibit two fundamental types of motion: spontaneous diffusion and drift induced by external forces. Drawing inspiration from these natural phenomena, we propose a novel search strategy to simulate the characteristics of particle motion, called the Particle Drift-Diffusion Process (*PDD_Process* for short). This search approach combines the two fundamental particle motions of drift and diffusion, achieving a balance between exploration and exploitation. The *PDD_Process* employs directed sampling operations along the two directions guided by guiding particles to simulate drift motion, and a gradually shrinking diffusion operator to simulate diffusion motion. The drift component generates directed motion along specific directions, while the diffusion component corresponds to the disordered motion of particles.

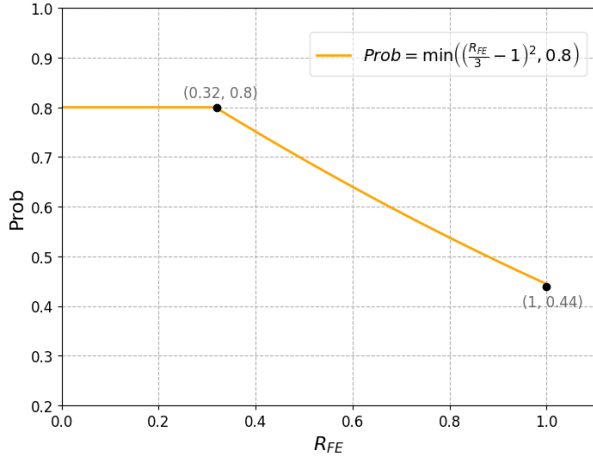


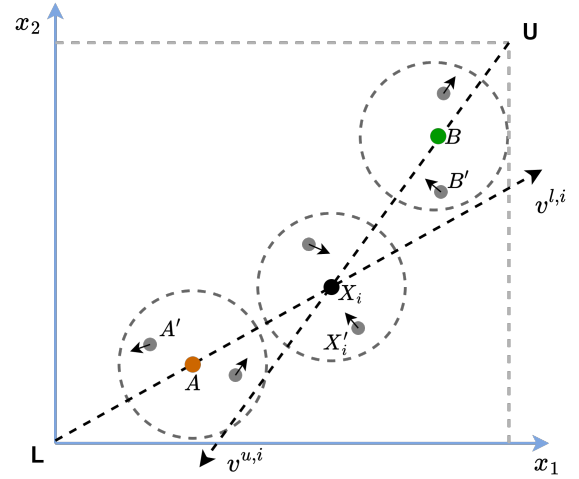
Fig. 2. Relationship between the triggering probability of the parameters $Prob$ and R_{FE} .

To simulate the adaptive adjustment of PDD_Process in response to environmental changes, we propose a dynamic modulation of the probability for triggering the PDD_Process. The calculation of the probability $Prob$ of triggering the PDD_Process is as follows:

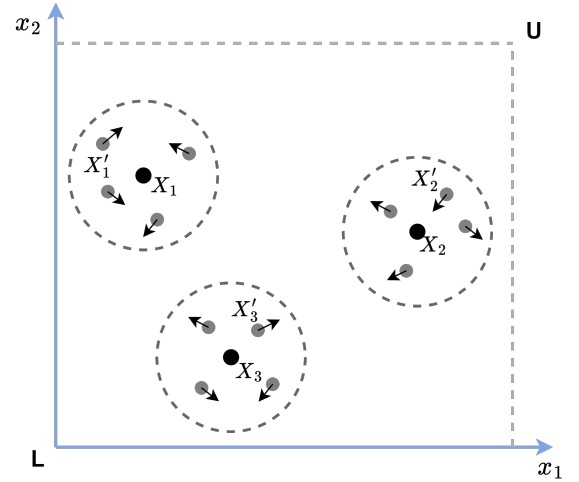
$$Prob = \min((R_{FE}/3 - 1)^2, U_p) \quad (8)$$

The relationship between $Prob$ and R_{FE} is illustrated in Fig. 2, assuming U_p is a fixed probability threshold of 0.8. When R_{FE} is between 0 and 0.32, $Prob$ remains at the upper bound of 0.8. However, as R_{FE} increases from 0.32 to 1, $Prob$ gradually decreases until reaching a lower bound of 0.44 when R_{FE} equals 1. In the early optimization stage, when R_{FE} is relatively small, a higher triggering probability (e.g., 0.8) is assigned to the PDD_Process, simulating the vigorous drift-diffusion motion of particles driven by high concentration gradients between regions. Conversely, in the later optimization stage, as R_{FE} increases, the triggering probability gradually decreases to a lower level (e.g., 0.44), mimicking the mild drift-diffusion behavior of particles in low concentration gradients.

The framework PDD divides the optimization process into three sub-stages: two coarse-tuning sub-stages and one fine-tuning sub-stage. Different strategies of drift-diffusion operations are performed according to the current sub-stage. During the coarse-tuning sub-stage, as depicted in Figure 3(a), we employ a directed sampling operation along two directions of the guiding particles to simulate drift motion, and a gradual shrinking diffusion operator to simulate diffusion motion. Points A and B represent the potential positions of particles obtained through drift along the two directions of the guiding particle X_i . Positions X'_i , A' , and B' correspond to the potential positions of particles generated by the diffusion of X_i , A , and B , respectively. During the fine-tuning stage, illustrated in Figure 3(b), the guiding particles solely undergo diffusion driven by the shrinking diffusion operator. The drift component helps avoid premature convergence to local optima and significantly augmenting the likelihood of intersecting the true PF. By enabling particles to move in directed trajectories,



(a)



(b)

Fig. 3. Particle drift-diffusion process. (a) depicts the coarse-tuning sub-stage process. (b) depicts the fine-tuning sub-stage process.

it facilitates a more expansive exploration of the decision space. Conversely, the disordered diffusion motion enhances local search capabilities of MOEAs within sub-regions. This random movement allows for a more thorough exploitation of local regions, refining solutions and enhancing the overall quality of the obtained Pareto set.

The pseudo-code of particle drift-diffusion process is shown in Algorithm 2. Firstly, the selection strategy of guiding particles is used to select $N_{w'} = \lceil N/10 \rceil$ guiding particles from the population P . The set X of guiding particles undergoes diffusion operator using Eq. (11) to obtain a diffusion solution set X_1^* . Then, check whether R_{FE} is below a threshold $Rate$. If so, the set X_d of drifting particles is generated for X using Eqs. (6-7), simulating drift motion of particles towards promising regions. The X_d undergoes a subsequent diffusion process using Eq. (11) to produce another diffusion set X_2^* . Finally, X_1^* and X_2^* are merged into the set Q .

Algorithm 3 Selection Strategy of Guiding Particles

Input: P (the population), $RefV$ (a set of reference vectors), $N_{w'}$ (the number of reference vectors after clustering)
Output: G (a set of guiding particles)

- 1: $S = \emptyset$
- 2: $RefV' = Kmeans(RefV, N_{w'})$
- 3: **for** $i = 1 : |P|$ **do**
- 4: Calculate the angle between the i -th individual and each reference vector of $RefV'$;
- 5: Assign the i -th individual to its closest reference vector that has the minimum angle between this individual and all reference vectors;
- 6: **end for**
- 7: **for** $i = 1 : N_{w'}$ **do**
- 8: **if** the reference vector $RefV'_i$ has been assigned to at least one individual **then**
- 9: Calculate IAPD for each individual assigned to this reference vector;
- 10: Select the individual with the minimum IAPD to G ;
- 11: **end if**
- 12: **end for**
- 13: **for** $i = 1 : N_{w'}$ **do**
- 14: **if** the reference vector $RefV'_i$ has not been assigned to any individual **then**
- 15: Sort the individuals within the population (excluding those already in G) in ascending order according to the value of IAPD;
- 16: Select the first individual and add it to G ;
- 17: **end if**
- 18: **end for**
- 19: **return** G

B. Selection Strategy of Guiding Particles

During the processes of particle drift and diffusion, individual particles exhibit varying degrees of influence. High-quality guiding particles can effectively steer the swarm towards promising regions, facilitating a more uniform distribution within these areas. In contrast, low-quality particles possess limited driving force and may even impede the overall progress of the evolutionary process. To more effectively allocate computational resources to these high-quality particles in optimization process, we propose a meticulously designed guiding particle selection strategy. This strategy aims to identify high-quality particles that can significantly enhance the performance of convergence and diversity.

Inspired by the APD, an improved angle-penalized distance calculation method (IAPD for short) is presented in this paper. As shown in Eq. (9), the key modification in IAPD replaces the term for calculating $P_{\theta_{i,j}}$ in the original Eq. (3) of APD.

$$P_{\theta_{i,j}} = M \cdot 0.1^{R_{FE}} \cdot \frac{\theta_{i,j}}{\gamma_{w_j}} \quad (9)$$

Different from the design concepts of APD, $P_{\theta_{i,j}}$ decreases over time in IAPD, controlled by the factor $0.1^{R_{FE}}$. This inverse operation means that IAPD initially places more emphasis on the diversity criterion $\theta_{i,j}$ and gradually shifts

Algorithm 4 Sub-stage Division

Input: $Rate$ (coarse-tuning rate)
Output: CSL (cumulative step length of sub-stages)

- 1: $CSL = \{0, 0, 0, 1\}$
- 2: **for** $k = 0 : 2$ **do**
- 3: $CSL(k) = (k - k^2/2^2) \cdot Rate$
- 4: **end for**
- 5: **return** CSL

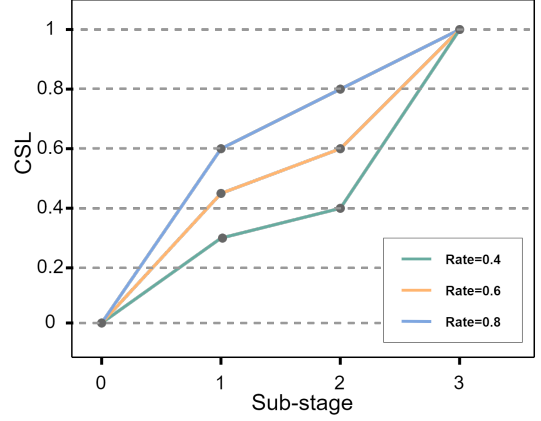


Fig. 4. The curves of CSL for the sub-stages corresponding to different values of $Rate$. The first and second sub-stages are the coarse-tuning sub-stages, and the third sub-stage is the fine-tuning sub-stage.

towards prioritizing the convergence criterion $\|f'_i\|$ as the optimization advances. In the particle drift and diffusion process, we desire the MOEAs to effectively explore the entire decision variable space while maintaining population diversity in the early stages. Therefore, IAPD initially places more emphasis on the diversity criterion $\theta_{i,j}$, allowing guiding particles to guide the population towards the PF. Subsequently, MOEAs need to focus on convergence in the later stages to ensure that the population approaches the PF. IAPD gradually reduces the penalty weight for diversity and increasingly emphasizes the convergence criterion $\|f'_i\|$.

The above IAPD method is integrated into the selection strategy of guiding particles to adaptively balance the performance of convergence and diversity during the optimization process. The pseudo-code for the selection strategy of guiding particles is given in Algorithm 3. First, the original reference vector $RefV$ is clustered into $N_{w'}$ clusters using the k -means clustering technique to obtain a new set of reference vectors $RefV'$ (line 2). All individuals within the population P are then assigned to their closest reference vector in $RefV'$ according to the minimum angle between individuals and all reference vectors $RefV'$ (lines 3-6). IAPDs of all assigned individuals are computed. And then, the individual with the minimum value of IAPD in each $RefV'$ is selected and added to the set G (lines 7-12). If any $RefV'$ is left unassigned, individuals within the population (excluding those already in G) will be sorted in ascending order based on the value of IAPD, and the first individual will be selected and added to G (lines 13-18). Finally, the algorithm returns the set G containing the selected guiding particles.

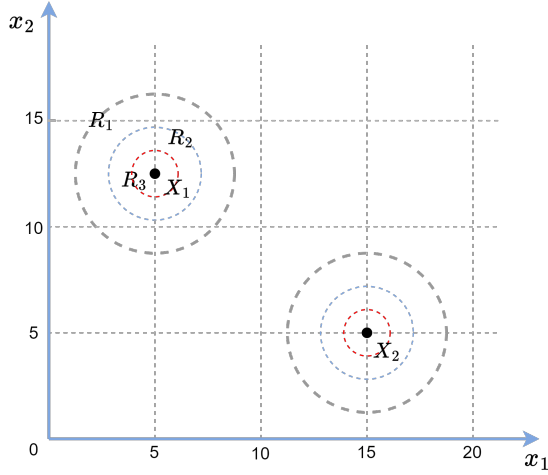


Fig. 5. An illustrative example of the gradual shrinking diffusion operator.

C. Sub-Stage Division

The proposed framework divides the entire optimization process into three sub-stages: the first two are the coarse-tuning sub-stages and the last one is the fine-tuning sub-stage. This division allows us to exert different driving forces on guiding particles according to the current sub-stage and implement refined operations on the particles. The mathematical expression of the sub-stage division method is as follows:

$$CSL(k) = \left(k - \frac{k^2}{22}\right) \cdot Rate, \quad k = 0, 1, 2 \quad (10)$$

where $CSL(k)$ represents the cumulative step length of the first k sub-stages. $Rate$ represents the proportion of coarse-tuning sub-stages in the entire optimization process. The value of $CSL(0)$ is set to 0 and $CSL(3)$ is set to 1 by default.

The pseudo-code for the division of sub-stages is given in Algorithm 4. To begin with, the cumulative step length of sub-stage array CSL is initialized. Finally, $CSL(k)$ is calculated using Eq. 10 (lines 3-5). The difference in the subtraction, i.e., $CSL(k) - CSL(k-1)$, specifically represents the interval length of the k -th sub-stage. The interval length represents the proportion of the search time for a particular sub-stage to the total time. As shown in Fig. 4, it can be observed that the interval length in the first sub-stage is larger than that in the second stage. When the PDD framework exhibits the poor performance of diversity, the value of $Rate$ should be increased to extend the time of the coarse-tuning sub-stage. Conversely, if it is found that the performance of convergence is unsatisfactory, reducing the $Rate$ of PDD is advisable. Generally, the value of $Rate$ parameters should be adjusted according to different problem scenarios.

D. Gradual Shrinking Diffusion Operator

Because of the significant concentration differences between the different regions, the particles exhibit a broad diffusion scope across other regions during the initial phase. As the diffusion process advances, these concentration differences gradually diminish and the diffusion range of particles gradually

TABLE I
FEATURES OF LSMOP TEST PROBLEMS

Problem	Features		
	Pareto frontier	Landscape	Separability
LSMOP1	Linear	Unimodal	Separable
LSMOP2	Linear	Mixed	Partially separable
LSMOP3	Linear	Multimodal	Mixed
LSMOP4	Linear	Mixed	Mixed
LSMOP5	Convex	Unimodal	Separable
LSMOP6	Convex	Mixed	Partially separable
LSMOP7	Convex	Multimodal	Mixed
LSMOP8	Convex	Mixed	Mixed
LSMOP9	Disconnected	Mixed	Separable

shrinks. Motivated by this phenomenon of particle diffusion, we propose a gradual shrinking diffusion operator to simulate the dynamic process of particle diffusion. The mathematical description of the gradual shrinking diffusion operator is as follows:

$$\begin{aligned} \Phi_k &= X_i - \mu^{k-1} \cdot \sigma_0 \\ \Psi_k &= X_i + \mu^{k-1} \cdot \sigma_0 \\ X_i^* &= Unif(\Phi_k, \Psi_k) \end{aligned} \quad (11)$$

where X_i represents an original particle, X_i^* represents the next position of the i -th particle, k represents the current k -th sub-stage, μ represents the shrinking rate, and σ_0 represents the initial deviation amplitude. Assuming that the diffusion motion falls within the interval $[\Phi_k, \Psi_k]$, the left and right endpoints of the interval $[\Phi_k, \Psi_k]$ can be calculated through μ and σ_0 . The function $Unif$ is used to generate uniformly distributed random numbers in the interval $[\Phi_k, \Psi_k]$. It is worth noting that μ and σ_0 should be set to different values to adapt to different problems.

To illustrate the process of gradual shrinking diffusion more clearly, we provide an example in a two-dimensional decision space. As shown in Fig. 5, the diffusion process for the original particles $x_1 = (5, 12.5)$ and $x_2 = (15, 5)$ is described as follows:

1) As can be seen from Eq. (11), assuming $\mu = 0.5$ and $\sigma_0 = 3$, we can obtain $\sigma_1 = 3$, $\sigma_2 = 1.5$, and $\sigma_3 = 0.75$, which correspond to the deviation amplitude for three sub-stages, respectively.

2) In Fig. 5, R_1 , R_2 , and R_3 correspond to the diffusion ranges of the k -th ($k = 1, 2, 3$) sub-stages, respectively. By adding the above σ_k to the original particles x_1 and x_2 , the diffusion range of particles can be determined, i.e., $x_1^* = \{(5 \pm 3, 12.5 \pm 3), (5 \pm 1.5, 12.5 \pm 1.5), (5 \pm 0.75, 12.5 \pm 0.75)\}$, and $x_2^* = \{(15 \pm 3, 5 \pm 3), (15 \pm 1.5, 5 \pm 1.5), (15 \pm 0.75, 5 \pm 0.75)\}$.

3) The next positions of particles are randomly generated through the $Unif$ function in Eq. (11).

The gradual shrinking diffusion operator makes use of the parameter k to determine which sub-stage the optimization process has arrived at. Subsequently, new solutions will be generated through varying diffusion ranges.

IV. EXPERIMENTAL STUDIES

In this section, comprehensive experiments are conducted on LSMOP [36], WFG [37] and ZDT [38] test suites to evaluate

TABLE II
PARAMETER SETTINGS FOR PDD AND COMPARISON
ALGORITHMS

General Settings	
Population Size	$N = 150(M = 2)$ $N = 200(M = 3)$
Termination Condition	$FE = 3 \times 10^5(M = 2)$ $FE = 5 \times 10^5(M = 3)$
Independent Runs	20
FDV	
Fuzzy Evolution Rate	0.8
Step Acceleration	0.4
LSMOF	
Weight Optimization Generation	10
Weight Optimization Population Size	30
WOF	
Number of Simplified Variants	4
Grouping Strategy	Ordered Grouping
Transformation Function	Interval Function
Original Problem Evaluations	1000
Transformed Problem Evaluations	500
PDD	
Initial Deviation Amplitude (σ_0)	3
Shrinking Rate (μ)	0.5
Coarse-Tuning Ratio (<i>Rate</i>)	0.6
Sampling Frequency (<i>S</i>)	5

the performance of the proposed PDD framework in solving LSMOPs. Experimental settings and result analysis can be found in the remaining parts of this section.

A. Experimental Settings

1) *Baseline Methods*: In order to investigate the effect of PDD on different types of MOEAs, four different types of MOEAs (NSGA-II [5], NSGA-III [6], LMOCSO [22], SMPSO [39]) are embedded into the proposed PDD framework for comprehensive performance comparisons on LSMOP test suite. These optimizers are chosen because they are widely used in the existing large-scale multi-objective optimization frameworks. The experimental comparisons involve three state-of-the-art frameworks of large-scale MOEAs mentioned in Section I, namely, FDV, LSMOF and WOF. Previous researches have demonstrated the effectiveness of these proposed frameworks in solving LSMOPs. The large-scale MOEAs are divided into four groups and compared with the corresponding PDD on the LSMOP test suites based on the embedded internal optimizer. By conducting comparative experiments with these frameworks, we evaluate the effectiveness of the proposed PDD framework in solving LSMOPs.

Then, LMOCSO is embedded in PDD framework (called PDD-LMOCSO) and compared with five state-of-the-art large-scale MOEAs (i.e., LMOEA-DS [30], ALMOEA [40], DGEA [24], CCGDE3 [13] and S^3 -CMA-ES [26]) on WFG and ZDT test suites.

2) *Benchmark Problems*: The benchmark test problems used in the experimental study are from LSMOP, WFG and ZDT test suites. First, the Pareto fronts in these benchmark LSMOP test suite have various geometrical shapes. The features of the nine test problems are given in Table I. LSMOP1-LSMOP4 have linear Pareto optimal frontiers (PF),

while LSMOP5-LSMOP9 have nonlinear variables. LSMOP5 - LSMOP8 have convex PFs, and LSMOP9 has a disconnected PF. The LSMOP test suite achieves a combination of different attribute landscapes in terms of modality and separability.

WFG test suite contains nine scalable problems, which have simpler landscapes and PFs than those in LSMOP test suite. There are some interactions between decision variables in the WFG problems, which poses challenges to MOEAs based on the grouping of decision variables. ZDT is one of the earliest multi-objective optimization test suite, which contains six bi-objective test problems with different PFs and landscapes. The number of decision variables in these benchmark problems is scalable.

3) *Parameter Settings*: In this study, comprehensive comparisons are performed between three state-of-the-art frameworks proposed for LSMOPs and our PDD. To ensure fair comparisons, all experiments are implemented using MATLAB code on PlatEMO v4.5 [41], following the parameter settings recommended in the literature. Table II summarizes the general and algorithm-specific parameter settings. The population size N and the maximum function evaluations FE are set to different values based on the number of objectives M . For $M = 2$, N is set to 150 and FE is set to 3×10^5 . For $M = 3$, N is set to 200 and FE is set to 5×10^5 . The value of perturbation deviation error (σ) and perturbation attenuation coefficient (μ) are set to 3 and 0.5, respectively. After investigating the influence of different values of *Rate* and *S* on the performance of PDD (refer to Section IV-C), the coarse-tuning ratio *Rate* is set to 0.6, and *S* is set to 5.

4) *Performance Metric*: To calculate IGD [42], [43] and HV [44] for all instances, reference points are obtained from the true PF samples of each problem. Each algorithm was run 20 times on each test problem independently, and the Wilcoxon rank-sum test [45] is conducted at a significance level of 0.05 to compare the results between our algorithm and other algorithms. The symbols “+”, “-”, and “ \approx ” denote that the compared algorithm is significantly better than, significantly worse than, or shows no statistically significant difference compared to our algorithm, respectively.

B. General Performance

In this section, different types of MOEAs (i.e. NSGA-II, NSGA-III, LMOCSO, and SMPSO) are embedded into our proposed PDD framework, called PDD-Alg (where “Alg” denotes the embedded algorithm). Subsequently, we categorize them into four groups based on the type of embedded optimizer and conduct comparative experiments.

1) *IGD Values*: In the first set of comparative experiments, NSGAII was embedded into FDV, LSMOF, WOF, and PDD as the internal optimizer. The IGD results obtained by the five comparative frameworks are summarized in Table III. Compared to the original NSGAII, the four frameworks embedded with NSGAII have made significant improvements in solving the LSMOP test suite. However, compared with other frameworks, our PDD shows superior overall performance. Specifically, PDD-NSGAII achieves the best results in 39 of 54 test problems, while the comparative frameworks that used

TABLE III
STATISTICS OF IGD RESULTS OBTAINED BY FIVE COMPARED METHODS WITH THE OPTIMIZER NSGAII ON 54 TEST INSTANCES FROM LSMOP TEST SUITE. THE BEST RESULT IS SHOWN IN BOLD FONT.

Problem	M	D	NSGAII				
			NSGAII	FDV-NSGAII	LSMOF-NSGAII	WOF-NSGAII	PDD-NSGAII
LSMOP1	2	1000	1.8396e+0 (2.12e-1) -	1.4608e+0 (2.34e-1) -	6.2699e-1 (2.08e-2) -	6.0722e-1 (3.53e-2) -	2.2148e-1 (3.33e-2)
		2000	3.5638e+0 (2.15e-1) -	3.3712e+0 (1.88e-1) -	6.3490e-1 (1.59e-2) -	5.9406e-1 (7.94e-2) -	2.6161e-1 (3.55e-2)
		5000	5.4692e+0 (1.54e-1) -	5.1453e+0 (1.60e-1) -	6.6484e-1 (1.67e-2) -	6.2002e-1 (3.58e-2) -	3.1419e-1 (2.14e-2)
	3	1000	2.5437e+0 (1.63e-1) -	2.3411e+0 (1.65e-1) -	4.6946e-1 (8.61e-3) -	4.3946e-1 (8.46e-2) ≈	3.7644e-1 (2.28e-2)
		2000	4.6619e+0 (1.83e-1) -	4.6437e+0 (1.89e-1) -	5.6295e-1 (6.52e-3) -	5.5735e-1 (4.33e-2) -	3.9300e-1 (1.16e-2)
		5000	6.5445e+0 (2.26e-1) -	8.4282e+0 (2.59e-1) -	6.1450e-1 (8.38e-3) -	6.1484e-1 (5.02e-2) -	3.9892e-1 (7.64e-3)
LSMOP2	2	1000	3.3740e-2 (5.15e-4) -	3.4521e-2 (4.01e-4) -	1.4902e-2 (1.13e-3) -	1.5806e-2 (1.68e-3) -	1.4381e-2 (6.16e-4)
		2000	1.9568e-2 (1.08e-4) -	2.0679e-2 (9.24e-5) -	1.1208e-2 (2.66e-4) -	1.0865e-2 (2.65e-4) -	1.0190e-2 (4.39e-4)
		5000	9.6702e-3 (7.58e-5) -	1.0098e-2 (8.58e-5) -	7.5349e-3 (2.04e-4) -	6.9970e-3 (2.43e-4) -	6.7541e-3 (2.14e-4)
	3	1000	5.2243e-2 (1.28e-3) ≈	5.1517e-2 (1.85e-3) ≈	5.5235e-2 (1.43e-3) -	5.4941e-2 (1.32e-3) -	5.1490e-2 (1.20e-3)
		2000	4.4607e-2 (1.91e-3) ≈	4.6605e-2 (2.13e-3) -	4.8332e-2 (2.92e-3) -	4.8061e-2 (2.80e-3) -	4.3868e-2 (1.37e-3)
		5000	4.1917e-2 (1.80e-3) -	4.1905e-2 (2.17e-3) ≈	4.4698e-2 (1.74e-3) -	4.3517e-2 (1.35e-3) -	4.0673e-2 (1.28e-3)
LSMOP3	2	1000	1.7489e+1 (1.40e+0) -	1.8189e+1 (1.32e+0) -	1.5729e+0 (5.57e-4) ≈	1.3532e+0 (2.04e-1) ≈	1.2837e+0 (2.17e-1)
		2000	2.1499e+1 (6.85e-1) -	2.1642e+1 (7.64e-1) -	1.5770e+0 (2.19e-4) ≈	1.5606e+0 (3.67e-2) -	1.5039e+0 (6.55e-2)
		5000	2.6215e+1 (7.04e-1) -	2.6450e+1 (6.45e-1) -	1.5792e+0 (1.87e-4) +	1.5864e+0 (1.66e-3) ≈	1.5856e+0 (7.07e-4)
	3	1000	9.9277e+0 (1.99e+0) -	9.0889e+0 (1.14e+0) -	8.0693e-1 (1.56e-2) +	8.5997e-1 (1.56e-3) ≈	8.6034e-1 (1.11e-3)
		2000	1.7301e+1 (3.40e+0) -	1.4741e+1 (2.49e+0) -	8.5474e-1 (6.21e-3) +	8.6060e-1 (4.38e-4) -	8.5936e-1 (5.10e-3)
		5000	1.9919e+1 (4.28e+0) -	1.9976e+1 (2.61e+0) -	8.6060e-1 (5.44e-5) ≈	8.6072e-1 (1.31e-6) ≈	8.5441e-1 (1.93e-2)
LSMOP4	2	1000	5.5561e-2 (1.01e-3) -	5.5677e-2 (9.32e-4) -	3.0259e-2 (1.19e-3) +	3.5328e-2 (1.66e-3) -	3.1209e-2 (6.71e-4)
		2000	3.3251e-2 (2.90e-4) -	3.7033e-2 (9.77e-4) -	2.1563e-2 (7.10e-4) ≈	2.4487e-2 (2.29e-3) -	2.1193e-2 (8.26e-4)
		5000	1.7613e-2 (1.07e-4) -	1.9201e-2 (1.79e-4) -	1.4698e-2 (9.54e-4) ≈	1.5936e-2 (5.87e-4) -	1.4346e-2 (6.62e-4)
	3	1000	1.0905e-1 (4.29e-3) +	1.1533e-1 (2.43e-3) ≈	1.3113e-1 (2.55e-3) -	1.2874e-1 (2.51e-3) -	1.1566e-1 (3.45e-3)
		2000	7.2136e-2 (2.11e-3) +	7.4471e-2 (2.28e-3) ≈	8.3160e-2 (2.27e-3) -	8.1808e-2 (1.85e-3) -	7.4759e-2 (1.82e-3)
		5000	5.0203e-2 (1.95e-3) ≈	5.0951e-2 (2.13e-3) -	5.4297e-2 (2.95e-3) -	5.2572e-2 (2.06e-3) -	4.9135e-2 (1.35e-3)
LSMOP5	2	1000	4.1817e+0 (3.91e-1) -	2.9596e+0 (1.24e+0) -	7.4209e-1 (1.15e-16) -	5.7373e-1 (1.49e-1) -	3.3946e-1 (3.65e-3)
		2000	1.1011e+1 (7.81e-1) -	6.6694e+0 (1.82e+0) -	7.4209e-1 (1.15e-16) -	6.2279e-1 (1.28e-1) -	3.7007e-1 (9.70e-3)
		5000	1.5163e+1 (4.63e-1) -	1.2268e+1 (4.83e-1) -	7.4209e-1 (1.15e-16) -	7.4204e-1 (1.94e-4) -	7.2459e-1 (7.73e-3)
	3	1000	6.4311e+0 (3.63e-1) -	5.2400e+0 (4.98e-1) -	5.2212e-1 (2.32e-2) -	5.2963e-1 (5.84e-3) -	4.9252e-1 (1.24e-2)
		2000	1.2785e+1 (5.82e-1) -	1.0274e+1 (5.48e-1) -	5.3984e-1 (2.82e-3) -	5.3666e-1 (4.71e-3) -	5.1948e-1 (3.56e-3)
		5000	1.7101e+1 (4.94e-1) -	1.8155e+1 (4.70e-1) -	5.4078e-1 (9.44e-6) -	5.3553e-1 (4.88e-3) -	5.2423e-1 (3.39e-3)
LSMOP6	2	1000	7.6403e-1 (3.86e-2) -	7.7080e-1 (1.31e-2) -	3.1243e-1 (2.53e-4) +	4.9971e-1 (1.37e-1) -	3.7538e-1 (3.29e-2)
		2000	7.5723e-1 (1.19e-4) -	7.4766e-1 (3.86e-2) -	3.0869e-1 (1.66e-4) +	6.1755e-1 (1.15e-1) -	3.5667e-1 (4.75e-2)
		5000	7.4774e-1 (4.98e-7) -	7.4774e-1 (3.93e-13) -	3.0700e-1 (2.82e-4) +	6.1648e-1 (1.17e-1) -	3.3500e-1 (4.53e-2)
	3	1000	1.5335e+2 (3.69e+1) -	1.0873e+2 (6.94e+1) -	7.1266e-1 (1.80e-2) +	1.3066e+0 (1.11e-3) -	1.2886e+0 (5.60e-2)
		2000	4.3532e+3 (1.05e+3) -	1.6086e+3 (8.51e+2) -	7.7281e-1 (4.79e-2) +	1.3202e+0 (1.36e-3) ≈	1.3197e+0 (1.02e-3)
		5000	1.5429e+4 (4.46e+3) -	1.4756e+4 (3.23e+3) -	7.6936e-1 (4.25e-2) +	1.3268e+0 (1.34e-3) ≈	1.2662e+0 (1.47e-1)
LSMOP7	2	1000	7.5526e+1 (1.76e+2) -	1.5036e+1 (1.46e+0) -	1.5087e+0 (6.69e-4) +	1.5122e+0 (8.27e-4) ≈	1.5117e+0 (8.09e-4)
		2000	5.5698e+3 (2.42e+3) -	6.2741e+2 (5.92e+1) -	1.5131e+0 (2.74e-4) +	1.5170e+0 (1.55e-3) ≈	1.5167e+0 (6.28e-4)
		5000	2.6740e+4 (1.68e+3) -	1.1715e+4 (1.22e+3) -	1.5154e+0 (2.61e-4) +	1.5207e+0 (1.55e-3) ≈	1.5196e+0 (3.92e-4)
	3	1000	1.1058e+0 (2.17e-3) -	1.0949e+0 (4.60e-3) -	8.6041e-1 (2.37e-3) -	8.5054e-1 (4.59e-3) -	8.4715e-1 (6.28e-4)
		2000	1.0191e+0 (1.01e-3) -	1.0185e+0 (2.62e-3) -	8.4772e-1 (1.22e-3) -	8.4302e-1 (8.50e-4) -	8.4092e-1 (4.45e-4)
		5000	9.7274e-1 (1.92e-4) -	9.7284e-1 (4.80e-4) -	8.4074e-1 (9.68e-4) -	8.3842e-1 (7.66e-4) -	8.3752e-1 (3.26e-4)
LSMOP8	2	1000	1.1963e+0 (6.96e-2) -	1.7236e+0 (2.32e-1) -	7.4209e-1 (1.15e-16) -	6.5854e-1 (1.43e-1) -	3.8151e-1 (5.40e-2)
		2000	4.3206e+0 (3.20e-1) -	5.1909e+0 (3.81e-1) -	7.4209e-1 (1.15e-16) -	6.9247e-1 (1.02e-1) -	4.0316e-1 (3.34e-2)
		5000	8.7214e+0 (2.41e-1) -	9.7380e+0 (3.28e-1) -	7.4209e-1 (1.15e-16) -	7.4030e-1 (4.89e-3) -	7.0194e-1 (1.95e-2)
	3	1000	4.8652e-1 (2.34e-2) -	8.2486e-1 (4.08e-2) -	3.3886e-1 (9.01e-3) -	3.0475e-1 (2.47e-2) -	1.4823e-1 (1.17e-2)
		2000	9.4416e-1 (3.78e-2) -	9.4843e-1 (1.89e-2) -	3.3969e-1 (1.63e-2) -	3.2084e-1 (2.82e-2) -	1.4131e-1 (8.83e-3)
		5000	9.3650e-1 (5.59e-2) -	9.2761e-1 (5.15e-2) -	3.2996e-1 (1.74e-2) -	3.0001e-1 (2.84e-2) -	1.4017e-1 (9.63e-3)
LSMOP9	2	1000	1.0062e+0 (1.68e-3) -	6.3503e-1 (3.86e-3) -	8.0694e-1 (9.43e-4) -	8.0822e-1 (1.88e-3) -	3.8194e-2 (6.28e-3)
		2000	1.0506e+0 (3.73e-2) -	1.0974e+0 (1.34e-1) -	8.0496e-1 (1.48e-3) -	7.9853e-1 (3.53e-2) -	7.3728e-2 (1.20e-2)
		5000	8.4305e+0 (5.82e-1) -	1.0933e+1 (1.29e+0) -	8.0376e-1 (1.59e-3) -	8.0576e-1 (2.21e-3) -	6.4880e-2 (3.13e-3)
	3	1000	1.4851e+0 (3.48e-1) -	1.0460e+0 (3.46e-1) -	1.1447e+0 (2.39e-4) -	1.1447e+0 (3.81e-4) -	5.8786e-1 (6.88e-5)
		2000	4.4584e+0 (3.99e-1) -	3.9413e+0 (4.63e-1) -	1.1443e+0 (3.11e-4) -	1.1445e+0 (3.51e-4) -	5.8759e-1 (8.61e-5)
		5000	2.1006e+1 (7.74e-1) -	2.3373e+1 (1.26e+0) -	1.1439e+0 (2.58e-4) -	1.1442e+0 (3.20e-4) -	5.8728e-1 (7.07e-5)
+ / - / ≈			2/49/3	1/50/4	13/36/5	0/45/9	-

the same internal optimizer, namely, FDV-NSGAII, LSMOF-NSGAII and WOF-NSGAII, obtain the best results in 0, 13 and 0 test problems, respectively. PDD-NSGAII outperforms FDV-NSGAII in 50 test problems, LSMOF-NSGAII in 36 test problems and WOF-NSGAII in 45 test problems, respectively.

In the second set of experiments using NSGAIII as the internal optimizer, as shown in Table IV, the four frameworks that embedded with NSGAIII exhibit significant improvements compared to the original NSGAIII when solving the LSMOP test suite. Our PDD-NSGAIII achieves the best results in 37 of 54 test problems, outperforming FDV in all 54 test

problems, LSMOF in 36 test problems and WOF in 48 test problems, respectively. Specifically, PDD-NSGAIII performs well in LSMOP1, LSMOP2, LSMOP5, LSMOP8, LSMOP9, and tri-objective LSMOP7. LSMOF-NSGAIII achieves the best results mainly in LSMOP6, tri-objective LSMOP3, and bi-objective LSMOP7.

In the grouping where SMPSO and LMOCSO are used as optimizers, as shown in Table V, PDD-SMPSO outperforms SMPSO in 53 of 54 test problems and PDD-LMOCSO outperforms LMOCSO in 52 test problems. LMOCSO only performs well in bi-objective LSMOP3, mainly because LMOCSO relies

TABLE IV
STATISTICS OF IGD RESULTS OBTAINED BY FIVE COMPARED METHODS WITH THE OPTIMIZER NSGAIII ON 54 TEST INSTANCES FROM LSMOP TEST SUITE. THE BEST RESULT IS SHOWN IN BOLD FONT.

Problem	M	D	NSGAIII				
			NSGAIII	FDV-NSGAIII	LSMOF-NSGAIII	WOF-NSGAIII	PDD-NSGAIII
LSMOP1	2	1000	1.7272e+0 (1.64e-1) -	1.2121e+0 (2.10e-1) -	5.8191e-1 (3.23e-2) -	6.0694e-1 (6.59e-2) -	2.8513e-1 (3.29e-2)
		2000	3.1652e+0 (1.66e-1) -	2.6928e+0 (2.63e-1) -	6.1836e-1 (3.20e-2) -	6.2205e-1 (3.77e-2) -	3.0050e-1 (2.46e-2)
		5000	4.8399e+0 (1.31e-1) -	4.4669e+0 (1.22e-1) -	6.4520e-1 (2.02e-2) -	6.0695e-1 (6.08e-2) -	3.2344e-1 (7.81e-3)
	3	1000	5.7703e-1 (3.25e-2) -	1.0108e+0 (2.09e-1) -	4.9999e-1 (1.07e-2) -	4.1151e-1 (8.98e-2) ≈	3.3626e-1 (9.07e-3)
		2000	1.1893e+0 (7.76e-2) -	2.3486e+0 (2.21e-1) -	5.7523e-1 (1.08e-2) -	5.4119e-1 (4.42e-2) -	3.4804e-1 (6.86e-3)
		5000	2.5117e+0 (8.24e-2) -	5.3974e+0 (3.35e-1) -	6.3078e-1 (1.55e-2) -	6.3516e-1 (3.56e-2) -	3.5992e-1 (5.39e-3)
LSMOP2	2	1000	2.9613e-2 (4.16e-4) -	3.4071e-2 (4.48e-4) -	9.4306e-3 (2.53e-4) ≈	1.1294e-2 (8.82e-4) -	9.2673e-3 (2.98e-4)
		2000	1.8625e-2 (7.84e-5) -	1.9329e-2 (2.10e-4) -	5.7152e-3 (1.18e-4) +	7.4430e-3 (5.65e-4) -	6.2761e-3 (1.18e-3)
		5000	8.7602e-3 (6.88e-5) -	9.4117e-3 (2.40e-5) -	3.6754e-3 (8.14e-5) ≈	4.4476e-3 (1.77e-4) -	3.7878e-3 (6.13e-4)
	3	1000	3.8874e-2 (1.22e-4) -	3.9928e-2 (6.34e-5) -	3.8875e-2 (7.66e-4) -	3.9899e-2 (5.04e-4) -	3.4688e-2 (2.39e-4)
		2000	3.2037e-2 (1.98e-5) -	3.2392e-2 (3.06e-5) -	3.2437e-2 (2.08e-4) -	3.2760e-2 (1.34e-4) -	3.0568e-2 (7.85e-5)
		5000	2.8775e-2 (1.33e-5) -	2.9035e-2 (1.64e-5) -	2.9015e-2 (5.41e-5) -	2.9140e-2 (4.85e-5) -	2.8422e-2 (4.77e-5)
LSMOP3	2	1000	2.3463e+1 (2.05e+0) -	2.2902e+1 (1.43e+0) -	1.5732e+0 (3.73e-4) ≈	1.4305e+0 (2.32e-1) ≈	1.3743e+0 (2.38e-1)
		2000	2.4455e+1 (1.18e+0) -	2.5390e+1 (1.23e+0) -	1.5778e+0 (6.65e-4) -	1.4925e+0 (1.17e-1) ≈	1.5591e+0 (4.75e-2)
		5000	3.6619e+1 (4.51e-1) -	2.8667e+1 (6.17e-1) -	1.5802e+0 (7.22e-4) +	1.5870e+0 (1.76e-3) -	1.5854e+0 (5.73e-4)
	3	1000	3.6264e+0 (3.47e-1) -	3.6079e+0 (8.84e-1) -	8.0620e-1 (2.16e-2) +	8.5194e-1 (2.16e-2) ≈	8.6066e-1 (1.89e-4)
		2000	7.2788e+0 (7.22e-1) -	6.1310e+0 (3.22e-1) -	8.4650e-1 (2.20e-2) +	8.5966e-1 (4.22e-3) ≈	8.6071e-1 (9.37e-6)
		5000	1.2241e+1 (3.22e-1) -	1.3863e+1 (4.33e-1) -	8.5897e-1 (6.57e-3) +	8.6072e-1 (1.02e-7) -	8.6069e-1 (2.75e-5)
LSMOP4	2	1000	4.1386e-2 (4.86e-4) -	5.4803e-2 (8.07e-4) -	2.6264e-2 (3.64e-4) +	2.9214e-2 (1.75e-3) -	2.6300e-2 (2.63e-3)
		2000	2.5244e-2 (1.81e-4) -	3.2980e-2 (2.63e-4) -	1.4693e-2 (3.50e-4) -	1.6793e-2 (1.17e-3) -	1.4557e-2 (1.98e-3)
		5000	1.3912e-2 (9.66e-5) -	1.7847e-2 (1.73e-4) -	7.1517e-3 (1.99e-4) -	8.4417e-3 (3.81e-4) -	6.9827e-3 (1.78e-4)
	3	1000	7.5368e-2 (3.16e-3) -	8.5751e-2 (7.19e-4) -	7.6530e-2 (2.17e-3) -	8.9097e-2 (2.73e-3) -	6.6018e-2 (2.77e-3)
		2000	5.3229e-2 (2.63e-4) -	5.7771e-2 (4.25e-4) -	5.2810e-2 (1.53e-3) -	5.6690e-2 (7.69e-4) -	4.3942e-2 (3.91e-4)
		5000	3.6588e-2 (8.21e-5) -	3.7498e-2 (8.83e-5) -	3.5711e-2 (5.19e-4) -	3.6105e-2 (6.07e-4) -	3.2173e-2 (1.42e-4)
LSMOP5	2	1000	2.9720e+0 (4.04e-1) -	2.2070e+0 (1.40e+0) -	7.4209e-1 (1.15e-16) -	6.5570e-1 (1.18e-1) -	3.7284e-1 (7.76e-2)
		2000	8.7140e+0 (5.05e-1) -	6.4060e+0 (1.25e+0) -	7.4209e-1 (1.15e-16) -	6.5463e-1 (1.26e-1) -	4.2688e-1 (4.75e-2)
		5000	1.4632e+1 (3.86e-1) -	1.1342e+1 (4.26e-1) -	7.4209e-1 (1.15e-16) -	7.3883e-1 (1.31e-2) -	7.2544e-1 (7.88e-3)
	3	1000	1.6710e+0 (3.22e-1) -	2.0607e+0 (7.54e-1) -	5.0090e-1 (5.76e-2) -	5.3665e-1 (5.20e-3) -	4.7729e-1 (1.35e-2)
		2000	3.6151e+0 (1.67e-1) -	5.4473e+0 (5.22e-1) -	5.3601e-1 (8.79e-3) -	5.3788e-1 (4.18e-3) -	4.9645e-1 (2.13e-2)
		5000	7.1605e+0 (2.64e-1) -	1.1483e+1 (6.41e-1) -	5.4041e-1 (2.46e-3) -	5.4097e-1 (1.90e-4) -	4.9281e-1 (2.00e-2)
LSMOP6	2	1000	7.7363e-1 (2.57e-4) -	7.7399e-1 (7.75e-4) -	3.1339e-1 (1.57e-3) +	5.3546e-1 (1.40e-1) -	3.6417e-1 (4.38e-2)
		2000	7.5705e-1 (7.36e-5) -	7.5733e-1 (5.93e-5) -	3.0889e-1 (1.57e-3) +	5.8215e-1 (1.36e-1) -	3.6292e-1 (6.12e-2)
		5000	7.4772e-1 (5.78e-6) -	7.4774e-1 (7.53e-6) -	3.0685e-1 (1.97e-4) +	6.0015e-1 (1.27e-1) -	3.4883e-1 (4.54e-2)
	3	1000	4.5958e+1 (2.60e+1) -	3.1330e+1 (3.78e+1) -	7.4603e-1 (6.87e-2) +	1.3048e+0 (2.04e-3) -	1.2991e+0 (1.17e-3)
		2000	1.1377e+3 (4.31e+2) -	9.2587e+2 (5.56e+2) -	8.0499e-1 (3.55e-2) +	1.3201e+0 (1.78e-3) -	1.3163e+0 (1.02e-3)
		5000	2.7507e+3 (4.55e+2) -	2.6221e+3 (3.61e+2) -	7.9516e-1 (8.94e-2) +	1.3305e+0 (1.27e-2) -	1.3256e+0 (7.98e-4)
LSMOP7	2	1000	6.9273e+1 (1.53e+2) -	2.0305e+1 (2.69e+0) -	1.5088e+0 (6.54e-4) +	1.5117e+0 (1.49e-3) ≈	1.5114e+0 (1.54e-3)
		2000	1.4661e+3 (1.83e+3) -	7.1913e+2 (1.02e+2) -	1.5132e+0 (4.40e-4) +	1.5169e+0 (9.91e-4) -	1.5160e+0 (7.37e-4)
		5000	1.7721e+4 (6.46e+3) -	9.0660e+3 (7.52e+2) -	1.5154e+0 (2.23e-4) +	1.5207e+0 (9.89e-4) -	1.5192e+0 (6.51e-4)
	3	1000	1.0953e+0 (1.74e-3) -	1.0939e+0 (1.55e-3) -	8.5530e-1 (1.29e-2) -	8.5143e-1 (5.58e-3) -	8.4795e-1 (6.53e-4)
		2000	1.0149e+0 (6.24e-4) -	1.0158e+0 (6.93e-4) -	8.5527e-1 (1.81e-2) -	8.6165e-1 (3.03e-2) -	8.4110e-1 (4.75e-4)
		5000	9.7181e-1 (8.26e-5) -	9.7187e-1 (1.38e-4) -	8.6701e-1 (2.94e-2) -	8.4787e-1 (2.03e-2) -	8.3730e-1 (3.29e-4)
LSMOP8	2	1000	9.4497e-1 (7.77e-2) -	1.6765e+0 (2.39e-1) -	7.4209e-1 (1.15e-16) -	7.0727e-1 (9.07e-2) -	3.9023e-1 (1.22e-1)
		2000	2.7635e+0 (1.39e-1) -	4.3271e+0 (3.15e-1) -	7.4209e-1 (1.15e-16) -	7.3414e-1 (3.18e-2) -	4.3776e-1 (8.54e-2)
		5000	6.8360e+0 (2.26e-1) -	8.9313e+0 (3.04e-1) -	7.4209e-1 (1.15e-16) -	7.4186e-1 (9.12e-4) -	6.8946e-1 (1.71e-2)
	3	1000	2.4927e-1 (1.02e-2) -	3.8808e-1 (4.71e-2) -	2.6961e-1 (3.39e-2) -	2.3098e-1 (5.03e-2) -	1.0884e-1 (6.98e-3)
		2000	5.7522e-1 (5.64e-3) -	6.3557e-1 (8.15e-3) -	2.7348e-1 (4.30e-2) -	2.3352e-1 (4.89e-2) -	1.0374e-1 (7.77e-3)
		5000	6.3240e-1 (5.85e-3) -	9.0602e-1 (1.58e-2) -	2.8829e-1 (4.68e-2) -	2.1457e-1 (4.48e-3) -	1.0445e-1 (7.84e-3)
LSMOP9	2	1000	1.0072e+0 (1.72e-3) -	6.3811e-1 (2.83e-3) -	8.0675e-1 (1.04e-3) -	8.0869e-1 (5.64e-4) -	8.3296e-2 (3.96e-3)
		2000	9.5029e-1 (1.64e-2) -	1.1768e+0 (1.27e-1) -	8.0485e-1 (6.06e-4) -	7.9826e-1 (3.68e-2) -	7.0272e-2 (2.83e-3)
		5000	6.8926e+0 (3.75e-1) -	8.7335e+0 (7.71e-1) -	8.0377e-1 (1.78e-3) -	8.0488e-1 (4.49e-3) -	6.4099e-2 (2.72e-3)
	3	1000	1.5207e+0 (3.09e-1) -	1.0590e+0 (3.10e-1) -	1.1603e+0 (3.87e-2) -	1.1458e+0 (1.97e-3) -	5.8881e-1 (2.30e-4)
		2000	4.3038e+0 (5.62e-1) -	3.1266e+0 (3.52e-1) -	1.1456e+0 (1.06e-3) -	1.1456e+0 (1.23e-3) -	5.8898e-1 (6.74e-4)
		5000	2.0588e+1 (1.80e+0) -	1.8666e+1 (1.69e+0) -	1.1456e+0 (1.00e-3) -	1.1454e+0 (3.70e-4) -	5.8897e-1 (4.00e-4)
+ / - / ≈			0/54/0	0/54/0	15/36/3	0/48/6	-

on information from the current particle swarm to update particle positions, which results in slower convergence speed.

For LSMOP test suite with different numbers of objectives and different scales, PDD series achieve IGD values mostly smaller than those of other competitive algorithms, indicating that the proposed framework is able to handle complex problems more effectively.

2) *Convergence and Diversity Analysis*: To visually display the performance of these algorithms on LSMOP test suite, Figs. 6 and 7 show the median IGD values of final non-dominated solutions obtained by different comparative algorithms on the same test problems. From Fig. 6, we can observe

that on bi-objective LSMOP1 with a continuous linear PF, the PDD series achieve a well-converged and diverse solution set across 1000, 2000, and 5000 decision variables, especially PDD-SMPSO and PDD-LMOCSO. FDV-NSGAII, SMPSO, and LMOCSO do not converge well and obtain lower-quality solutions than those of PDD series. WOF-NSGAII and LSMOF-NSGAII achieve the intermediate quality of the solution set. On bi-objective LSMOP9 with a disjoint PF, most algorithms except SMPSO and LMOCSO achieve well-converged and diverse solutions.

Fig. 7 show that the PDD series obtain well-converged and diverse solution sets for tri-objective LSMOP8 and LSMOP9

TABLE V
STATISTICS OF IGD RESULTS OBTAINED BY TWO COMPARED METHODS WITH THE OPTIMIZERS SMPSO AND LMOCSO ON 54 TEST INSTANCES FROM LSMOP SUITE. THE BEST RESULT IS SHOWN IN BOLD FONT.

Problem	M	D	SMPSO		LMOCSO	
			SMPSO	PDD-SMPSO	LMOCSO	PDD-LMOCSO
LSMOP1	2	1000	1.5648e+0 (4.44e-2)	2.8304e-1 (2.43e-3)	5.2847e-1 (5.66e-2)	2.1871e-1 (2.22e-3)
		2000	1.6540e+0 (7.21e-2)	2.9792e-1 (1.51e-3)	1.3450e+0 (8.44e-2)	2.7171e-1 (4.68e-3)
		5000	1.7158e+0 (4.79e-2)	3.0466e-1 (5.37e-4)	2.0203e+0 (1.34e-1)	3.0061e-1 (4.67e-3)
	3	1000	1.9540e+0 (1.28e-1)	3.5886e-1 (5.72e-3)	9.0327e-1 (4.90e-2)	3.0211e-1 (3.67e-3)
		2000	2.1000e+0 (2.60e-1)	3.5906e-1 (5.29e-3)	1.3084e+0 (5.32e-2)	3.2925e-1 (5.55e-3)
		5000	2.1151e+0 (2.92e-1)	3.6013e-1 (5.40e-3)	1.5184e+0 (5.70e-2)	3.4437e-1 (6.74e-3)
LSMOP2	2	1000	2.3491e-2 (3.26e-4)	7.6240e-3 (2.10e-4)	2.2492e-2 (2.78e-4)	6.2036e-3 (1.22e-4)
		2000	1.3513e-2 (2.56e-4)	5.0376e-3 (1.29e-4)	1.2847e-2 (3.00e-4)	4.1183e-3 (3.46e-5)
		5000	7.3358e-3 (1.94e-4)	3.7238e-3 (1.06e-4)	6.4833e-3 (1.19e-4)	2.9205e-3 (1.22e-5)
	3	1000	4.7565e-2 (1.36e-3)	4.0718e-2 (1.64e-3)	3.5060e-2 (1.54e-4)	3.0262e-2 (6.95e-5)
		2000	4.1426e-2 (1.16e-3)	3.9056e-2 (1.44e-3)	3.0834e-2 (1.03e-4)	2.8673e-2 (5.21e-5)
		5000	3.9145e-2 (1.15e-3)	3.8334e-2 (1.79e-3)	2.8827e-2 (3.98e-5)	2.7867e-2 (1.25e-5)
LSMOP3	2	1000	2.7498e+1 (6.56e-1)	1.5668e+0 (6.72e-4)	7.3606e-1 (8.99e-3)	1.2496e+0 (5.92e-2)
		2000	2.8304e+1 (3.43e-1)	1.5730e+0 (6.63e-4)	1.2350e+0 (1.95e-1)	1.5161e+0 (3.24e-2)
		5000	2.8831e+1 (2.43e-1)	1.5759e+0 (4.32e-4)	7.6489e+0 (1.90e+0)	1.5864e+0 (4.29e-4)
	3	1000	1.3618e+1 (2.74e+0)	8.4720e-1 (2.80e-2)	7.6742e+0 (3.32e+0)	8.2209e-1 (3.71e-2)
		2000	1.2759e+1 (1.65e+0)	8.5942e-1 (3.81e-3)	1.0997e+1 (1.59e+0)	8.5970e-1 (3.96e-3)
		5000	1.3879e+1 (2.55e+0)	8.5227e-1 (2.04e-2)	1.2473e+1 (2.52e+0)	8.5871e-1 (5.75e-3)
LSMOP4	2	1000	5.0685e-2 (4.14e-4)	2.1342e-2 (1.88e-4)	4.8020e-2 (5.49e-4)	1.8247e-2 (4.05e-4)
		2000	3.0218e-2 (2.36e-4)	1.1911e-2 (1.41e-4)	2.8691e-2 (2.02e-4)	1.0956e-2 (1.40e-4)
		5000	1.5098e-2 (1.30e-4)	6.3204e-3 (1.17e-4)	1.4138e-2 (4.76e-5)	5.5380e-3 (5.37e-5)
	3	1000	1.0595e-1 (1.85e-3)	6.4975e-2 (1.13e-3)	8.4968e-2 (5.06e-4)	5.2298e-2 (5.76e-4)
		2000	6.7880e-2 (1.29e-3)	4.8440e-2 (1.46e-3)	5.3761e-2 (1.53e-4)	3.7761e-2 (1.84e-4)
		5000	4.6192e-2 (1.13e-3)	4.0861e-2 (1.12e-3)	3.5478e-2 (5.15e-5)	3.0274e-2 (6.41e-5)
LSMOP5	2	1000	3.0714e+0 (2.77e-1)	7.4209e-1 (1.15e-16)	1.0521e+0 (1.21e-1)	3.5909e-1 (1.32e-2)
		2000	3.6947e+0 (1.16e-1)	7.4209e-1 (1.15e-16)	3.1546e+0 (3.73e-1)	7.3902e-1 (4.06e-3)
		5000	3.8799e+0 (1.61e-1)	7.4209e-1 (1.15e-16)	4.7126e+0 (4.46e-1)	7.4209e-1 (1.15e-16)
	3	1000	4.4116e+0 (2.90e-1)	5.0952e-1 (5.08e-3)	1.8031e+0 (1.39e-1)	3.2428e-1 (1.24e-2)
		2000	4.4356e+0 (4.17e-1)	5.1244e-1 (8.85e-3)	2.7226e+0 (1.02e-1)	4.0021e-1 (1.29e-2)
		5000	4.2274e+0 (3.51e-1)	5.1557e-1 (5.36e-3)	3.3745e+0 (1.58e-1)	4.7950e-1 (2.56e-3)
LSMOP6	2	1000	7.5765e-1 (8.07e-4)	1.7889e-1 (4.76e-3)	7.5050e-1 (4.93e-2)	2.2275e-1 (4.17e-2)
		2000	7.4982e-1 (8.13e-4)	1.7315e-1 (6.64e-3)	7.5485e-1 (1.29e-3)	2.5188e-1 (5.14e-2)
		5000	7.4510e-1 (3.76e-4)	1.6975e-1 (8.47e-3)	7.4740e-1 (2.16e-4)	2.5024e-1 (4.73e-2)
	3	1000	1.9151e+3 (7.62e+2)	1.1307e+0 (1.92e-1)	1.5357e+1 (7.40e+0)	7.7624e-1 (1.85e-1)
		2000	2.1733e+3 (6.76e+2)	1.1665e+0 (2.30e-1)	1.4183e+2 (4.20e+1)	9.4744e-1 (2.82e-1)
		5000	2.1209e+3 (7.34e+2)	1.1634e+0 (2.08e-1)	4.8419e+2 (1.04e+2)	9.0795e-1 (2.18e-1)
LSMOP7	2	1000	9.6160e+2 (1.28e+2)	1.5109e+0 (5.81e-4)	3.7193e+1 (2.63e+1)	1.5106e+0 (1.75e-3)
		2000	1.5791e+3 (1.35e+2)	1.5142e+0 (2.32e-4)	1.0499e+3 (5.15e+2)	1.5164e+0 (1.42e-3)
		5000	2.0910e+3 (2.43e+2)	1.5161e+0 (2.52e-4)	4.6014e+3 (1.31e+3)	1.5197e+0 (6.70e-4)
	3	1000	1.0787e+0 (1.41e-3)	8.1270e-1 (5.61e-2)	9.9356e+1 (9.08e-2)	8.4081e-1 (8.02e-4)
		2000	1.0067e+0 (4.93e-4)	8.1080e-1 (5.62e-2)	9.0625e+1 (9.30e-2)	8.3964e-1 (4.98e-4)
		5000	9.6837e-1 (9.01e-5)	7.8964e-1 (6.22e-2)	9.2744e-1 (4.44e-2)	8.3741e-1 (3.93e-4)
LSMOP8	2	1000	2.4536e+0 (2.25e-1)	5.5465e-1 (2.30e-2)	9.9983e-1 (1.51e-1)	2.5363e-1 (4.22e-3)
		2000	2.8920e+0 (1.80e-1)	7.4209e-1 (1.15e-16)	2.6211e+0 (3.67e-1)	5.2941e-1 (1.90e-2)
		5000	2.9900e+0 (1.38e-1)	7.4209e-1 (1.15e-16)	3.8529e+0 (4.47e-1)	7.4209e-1 (1.15e-16)
	3	1000	7.2807e-1 (6.00e-2)	8.7876e-2 (4.21e-3)	5.2218e-1 (7.59e-3)	5.8586e-2 (1.37e-3)
		2000	6.8110e-1 (4.35e-2)	8.3779e-2 (3.30e-3)	5.1596e-1 (3.93e-3)	6.1709e-2 (9.82e-4)
		5000	6.5513e-1 (4.97e-2)	8.1644e-2 (2.46e-3)	5.1604e-1 (6.67e-3)	6.4028e-2 (1.05e-3)
LSMOP9	2	1000	1.2206e+0 (1.56e-1)	3.2784e-2 (6.04e-4)	4.9116e-1 (5.07e-2)	3.4817e-2 (3.63e-3)
		2000	1.8933e+0 (3.08e-1)	1.8869e-2 (6.28e-4)	1.2949e+0 (2.55e-1)	2.3576e-2 (6.69e-3)
		5000	1.8540e+0 (2.69e-1)	1.1064e-2 (4.15e-4)	7.2373e+0 (1.95e+0)	1.6899e-2 (4.78e-3)
	3	1000	1.8060e+1 (1.06e+0)	5.7324e-1 (2.07e-3)	6.8320e-1 (1.05e-1)	5.9297e-1 (1.23e-4)
		2000	2.3162e+1 (9.90e-1)	5.7232e-1 (1.25e-3)	7.1153e-1 (2.91e-2)	5.9328e-1 (8.78e-4)
		5000	2.4509e+1 (8.97e-1)	5.7235e-1 (1.44e-3)	1.1893e+0 (2.50e-1)	5.9309e-1 (4.17e-4)
		+/- / ≈	0.53/1	-	2.5/20	-

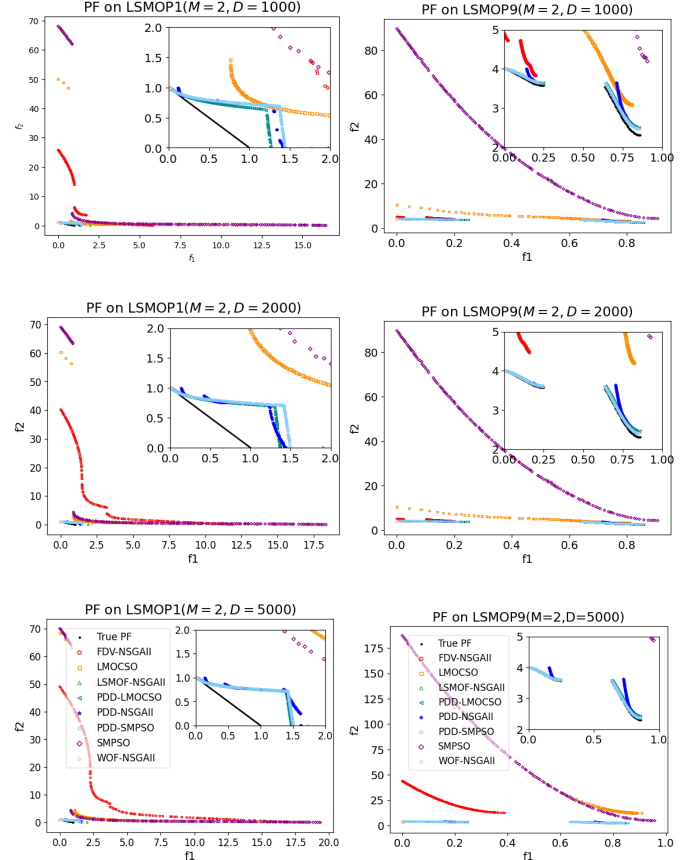


Fig. 6. Final solution sets are obtained by 8 compared methods on bi-objective LSMOP1 and LSMOP9 with different dimensions, and the true PFs are indicated by the black line.

with 5000 decision variables. Specifically, for the convex PF of tri-objective LSMOP8, the PDD series significantly improve the convergence and diversity of the solution sets compared to the original NSGAI, NSGAI, SMPSO, and LMOCSO. PDD-SMPSO and PDD-LMOCSO obtain a set of high-quality solutions. The final solutions of LSMOF and WOF series are unevenly distributed on PFs, and the FDV series exhibit poor convergence. On the disconnected PF of tri-objective LSMOP9, most comparative algorithms achieve good convergence, such as the LSMOF series and the WOF series. However, the final solution sets from these algorithms lack diversity because of limited evaluations. In such cases, the PDD series achieve a better distribution of solutions compared to other algorithms.

C. Compared with State-of-the-Art Large-Scale MOEAs

In this section, in order to analyze and evaluate the performance of PDD in solving different LSMOPs, LMOCSO is embedded into PDD (called PDD-LMOCSO). PDD-LMOCSO is compared with other most representative and state-of-the-art large-scale MOEAs (i.e., LMOEA-DS, ALMOEA, DGEA, CCGDE3 and S^3 -CMA-ES), including the WFG and ZDT test suites from 1000 up to 5000 dimensions. The experimental results obtained by these comparative algorithms are shown in Tables VI and VII.

1) *WFG*: In the WFG test suite, the IGD results of PDD-LMOCSO are compared with three other MOEAs (i.e. LMOEA-DS, ALMOEA, and DGEA), as shown in Table VI. Overall, the performance of PDD-LMOCSO is comparable to LMOEA-DS but significantly better than ALMOEA and DGEA. Specifically, PDD-LMOCSO, LMOEA-DS, ALMOEA, and DGEA achieve the best results in 23, 24, 6 and 1 of 54 test problems, respectively. PDD-LMOCSO outperforms LMOEA-DS in 18 instances, ALMOEA in 48 instances, and DGEA in 45 instances, respectively. It is worth noting that PDD-LMOCSO is slightly inferior to LMOEA-DS in WFG1, WFG3, WFG4, WFG7 and bi-objective WFG5, but the overall difference is not significant.

2) *ZDT*: In the ZDT test suite, the IGD results of PDD-LMOCSO are compared with three other MOEAs (i.e. LMOEA-DS, CCGDE3, and S^3 -CMA-ES), as shown in Table VII. The overall performance of PDD-LMOCSO is significantly better than LMOEA-DS, ALMOEA, and DGEA. Specifically, PDD-LMOCSO achieves the best results in 11 of 15 test problems. PDD-LMOCSO outperforms LMOEA-DS in 11 instances and surpasses both CCGDE3 and S^3 -CMA-ES in all 15 instances. It is worth noting that although the performance of LMOEA-DS is roughly equivalent to PDD-LMOCSO on the WFG test suite, it lags significantly behind

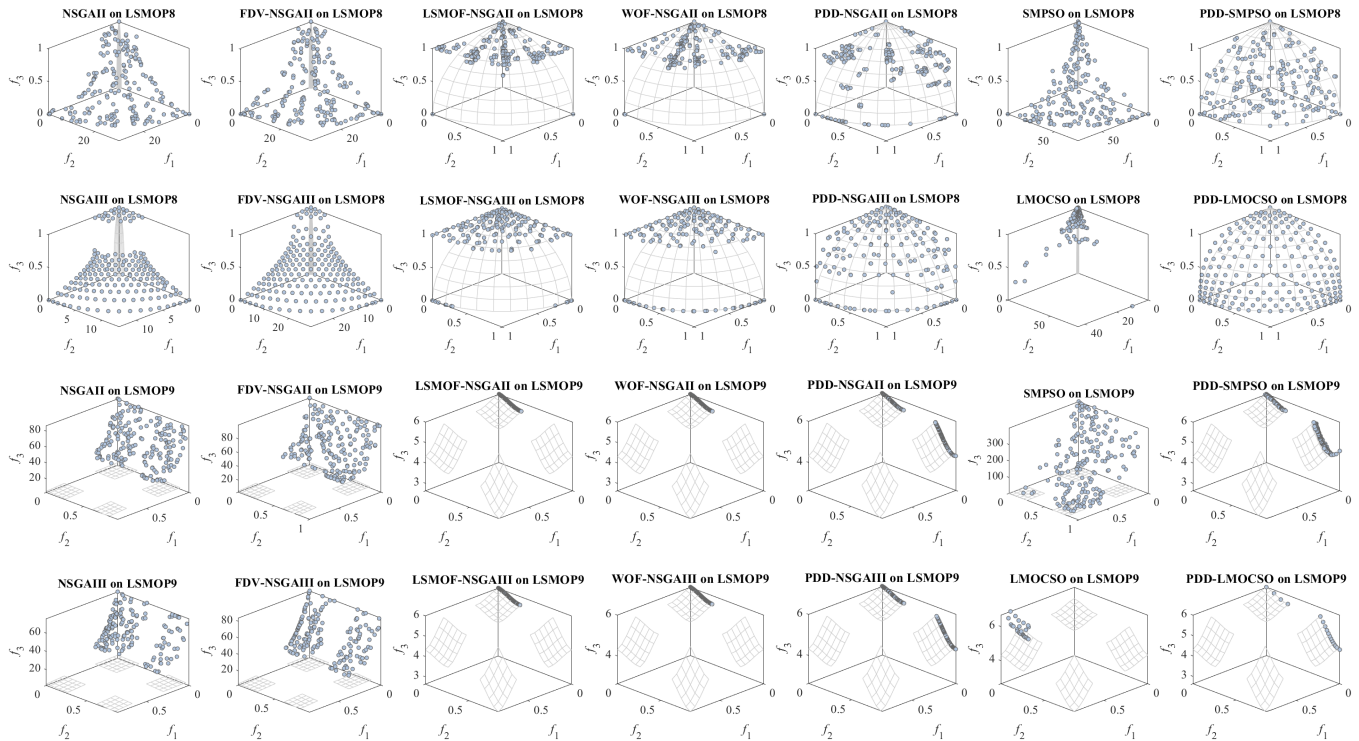


Fig. 7. Final solution sets are obtained by 14 compared methods on tri-objective LSMOP8 and LSMOP9 with 5000 decision variables, and the true PFs are indicated by the dash area.

PDD-LMOCSSO on the ZDT test suite.

D. Parameter Sensitivity Analysis

In this section, parameter sensitivity analysis is conducted to investigate the impact of parameters on the performance of PDD. The tested parameters are the coarse-tuning ratio ($Rate$) and the sampling frequency (S). Each parameter is set to four incremental values while keeping other parameters constant. Sensitivity experiments are performed on LSMOP test suite with bi-objectives and 1000 decision variables using PDD-NSGAIH and PDD-SMPSO. Each instance was independently run 20 times on all test problems. Friedman's test [45] was employed to compare the significant differences among different values of $Rate$ or S . As shown in Tables VIII and IX, the average rankings at the bottom of the tables display the average rankings based on IGD values for all test problems across the four instances. Lower rankings indicate better performance.

1) *Coarse-Tuning Ratio ($Rate$)*: $Rate$ is used to adjust the proportion of coarse-tuning sub-stage during the entire optimization process, and it is set as $Rate = [0.2, 0.4, 0.6, 0.8]$ for sensitivity analysis.

As shown in Table VIII, it can be observed that PDD embedded with NSGAIH performs better at a higher value of $Rate$, while PDD embedded with SMPSO performs better at a lower value of $Rate$. This is because NSGAIH retains elite solutions in each generation, making it prone to local optima in large-scale problems. A higher value of $Rate$ will increase the time for coarse-tuning optimization, which helps to obtain more diverse solutions and thus assist the population

in escaping from local optima. On the other hand, SMPSO has good diversity but weaker convergence performance. A lower value of $Rate$ will increase the time for fine-tuning optimization, strengthening the capability of local search and improving the performance of convergence. These indicate that different values of $Rate$ should be set according to the characteristics of embedded MOEAs to balance convergence and diversity. In general, to satisfy the performance of most algorithms, the value of $Rate$ is recommended to be set between 0.4 and 0.6.

2) *Sampling Frequency (S)*: S controls the drifting times at which particles undergo directed sampling along the two search directions. The values of S are set as 2, 5, 8, and 10, respectively for sensitivity analysis. The optimal value of S , similar to $Rate$, depends on the optimizer embedded in PDD. As shown in Table IX, it can be observed that PDD embedded with NSGAIH performs well on the test problems in the interval of $S = [5, 10]$. On the other hand, PDD embedded with SMPSO achieves the best performance with $S = 2$. In most cases, it is recommended to use $S = [4, 8]$ for PDD embedded with different optimizers.

E. Computational Efficiency

To further investigate the computational efficiency of PDD, we present a bar chart in Fig. 8 displaying the average computational time of 14 comparative algorithms on bi-objective and tri-objective LSMOP1-LSMOP9 problems with 1000 decision variables. It can be observed that the average computation time of the PDD series, embedded with different solvers, is

TABLE VI
STATISTICS OF IGD RESULTS OBTAINED BY FOUR COMPARED ALGORITHMS ON 54 TEST INSTANCES FROM WFG TEST SUITE. THE BEST RESULT IS SHOWN IN BOLD FONT.

Problem	M	D	LMOEA-DS	ALMOEA	DGEA	PDD-LMOCSO
WFG1	2	1000	1.0897e+0 (3.94e-2) +	1.5754e+0 (3.53e-2) -	1.2914e+0 (1.01e-2) -	1.1746e+0 (2.79e-2)
		2000	1.1064e+0 (5.26e-2) ≈	1.5934e+0 (1.05e-2) -	1.2947e+0 (8.00e-3) -	1.1225e+0 (5.03e-2)
		5000	1.0959e+0 (2.41e-2) ≈	1.5806e+0 (2.54e-2) -	1.2915e+0 (7.15e-3) -	1.1353e+0 (2.69e-2)
	3	1000	1.2395e+0 (1.77e-1) +	1.3683e+0 (2.64e-2) -	1.5164e+0 (7.93e-3) -	1.3650e+0 (2.22e-2)
		2000	1.2916e+0 (8.75e-2) ≈	1.8722e+0 (1.19e-2) -	1.5206e+0 (7.09e-3) -	1.3522e+0 (1.43e-2)
		5000	1.2760e+0 (9.45e-2) ≈	1.8464e+0 (1.28e-2) -	1.5278e+0 (1.00e-2) -	1.3157e+0 (3.88e-2)
WFG2	2	1000	6.0370e-2 (1.33e-2) ≈	4.5216e-1 (1.32e-2) -	2.9811e-1 (9.53e-3) -	5.2510e-2 (1.12e-2)
		2000	6.5477e-2 (1.35e-2) ≈	4.6030e-1 (2.09e-2) -	3.1889e-1 (2.11e-2) -	4.5123e-2 (1.34e-2)
		5000	7.9756e-2 (5.63e-3) -	4.5586e-1 (1.10e-2) -	3.1563e-1 (1.89e-2) -	2.8081e-2 (8.27e-3)
	3	1000	2.0046e-1 (8.96e-3) -	6.2458e-1 (7.49e-2) -	4.0431e-1 (1.97e-2) -	1.4257e-1 (8.48e-3)
		2000	1.9204e-1 (1.49e-2) -	6.2580e-1 (7.88e-2) -	4.2734e-1 (1.31e-2) -	1.4430e-1 (1.53e-2)
		5000	1.9897e-1 (1.32e-2) -	6.3501e-1 (5.12e-2) -	4.2067e-1 (1.57e-2) -	1.3392e-1 (1.05e-2)
WFG3	2	1000	6.5822e-2 (7.03e-3) ≈	5.1904e-1 (9.07e-3) -	3.4598e-1 (1.31e-2) -	7.5632e-2 (8.19e-3)
		2000	6.9182e-2 (6.72e-3) ≈	5.2260e-1 (1.36e-2) -	3.8345e-1 (1.58e-2) -	7.6601e-2 (1.42e-2)
		5000	7.2387e-2 (2.33e-3) ≈	5.2184e-1 (1.38e-2) -	3.8139e-1 (2.47e-2) -	5.9526e-2 (2.34e-2)
	3	1000	8.9273e-2 (8.23e-3) +	5.2558e-1 (4.73e-2) -	3.6758e-1 (5.97e-2) -	1.2220e-1 (3.38e-3)
		2000	8.3452e-2 (8.12e-3) +	5.3308e-1 (4.12e-2) -	3.6541e-1 (3.83e-2) -	1.2094e-1 (1.92e-3)
		5000	8.7956e-2 (8.74e-3) +	5.4981e-1 (3.60e-2) -	3.3596e-1 (4.00e-2) -	1.2091e-1 (4.75e-3)
WFG4	2	1000	5.0617e-2 (6.90e-3) +	2.8591e-1 (4.52e-3) -	1.8429e-1 (7.17e-3) -	6.9914e-2 (3.66e-3)
		2000	5.7440e-2 (2.42e-3) +	2.8073e-1 (1.53e-2) -	1.9256e-1 (5.31e-3) -	8.0315e-2 (2.47e-3)
		5000	6.9841e-2 (5.75e-3) +	2.8504e-1 (1.13e-2) -	2.0227e-1 (7.33e-3) -	8.6005e-2 (3.71e-3)
	3	1000	1.6558e-1 (3.61e-3) +	4.4534e-1 (1.07e-2) -	2.8352e-1 (1.09e-2) -	1.8991e-1 (1.55e-3)
		2000	1.7389e-1 (3.00e-3) +	4.4135e-1 (1.07e-2) -	2.8163e-1 (5.73e-3) -	1.9448e-1 (2.25e-3)
		5000	1.8120e-1 (3.83e-3) +	4.3547e-1 (1.56e-2) -	2.7976e-1 (6.57e-3) -	1.9705e-1 (1.23e-3)
WFG5	2	1000	4.9466e-2 (1.50e-2) +	6.6950e-2 (1.33e-4) -	6.2646e-2 (1.92e-5) ≈	6.2695e-2 (1.33e-4)
		2000	5.9525e-2 (2.10e-3) +	6.5083e-2 (3.07e-5) -	6.2664e-2 (1.23e-4) ≈	6.2727e-2 (1.05e-4)
		5000	6.2299e-2 (7.79e-4) ≈	6.3746e-2 (2.77e-5) -	6.2638e-2 (1.91e-5) ≈	6.2661e-2 (4.79e-5)
	3	1000	1.3183e-1 (5.79e-3) -	1.6719e-1 (1.33e-4) +	1.7532e-1 (1.03e-3) -	1.7397e-1 (3.07e-4)
		2000	1.8121e-1 (8.41e-3) -	1.6599e-1 (4.56e-4) +	1.7707e-1 (2.28e-3) -	1.7397e-1 (3.70e-4)
		5000	1.7937e-1 (9.96e-3) -	1.6545e-1 (4.54e-4) +	1.7589e-1 (5.25e-4) -	1.7368e-1 (4.21e-4)
WFG6	2	1000	9.8467e-3 (5.75e-4) -	1.6566e-2 (3.14e-4) -	9.5094e-3 (1.82e-4) -	8.9141e-3 (1.93e-4)
		2000	9.0549e-3 (2.98e-4) -	1.2023e-2 (3.20e-4) -	9.3673e-3 (6.06e-4) -	8.7505e-3 (3.83e-5)
		5000	9.8801e-3 (7.85e-4) ≈	9.5606e-3 (9.46e-5) -	8.8304e-3 (9.34e-5) -	8.7194e-3 (5.78e-6)
	3	1000	1.7186e-1 (8.50e-3) -	1.5564e-1 (1.01e-3) +	1.6075e-1 (2.29e-4) ≈	1.6062e-1 (3.94e-5)
		2000	1.6997e-1 (7.51e-3) -	1.5081e-1 (3.61e-4) +	1.6164e-1 (1.31e-3) ≈	1.6065e-1 (3.84e-5)
		5000	1.6877e-1 (8.25e-3) ≈	1.4845e-1 (1.35e-4) +	1.6111e-1 (6.01e-4) -	1.6064e-1 (3.74e-5)
WFG7	2	1000	2.8640e-2 (1.57e-3) +	4.1056e-1 (1.19e-2) -	2.8057e-1 (9.53e-3) -	5.6566e-2 (7.45e-3)
		2000	3.8726e-2 (2.33e-3) +	4.1029e-1 (6.96e-3) -	3.0212e-1 (8.75e-3) -	3.9806e-2 (1.81e-2)
		5000	4.8567e-2 (1.14e-3) ≈	4.2269e-1 (8.07e-3) -	3.1678e-1 (2.85e-3) -	4.6430e-2 (3.24e-3)
	3	1000	1.6161e-1 (5.35e-3) -	6.0898e-1 (1.96e-2) -	3.7743e-1 (1.89e-2) -	1.7036e-1 (2.42e-3)
		2000	1.6944e-1 (5.27e-3) ≈	6.0547e-1 (2.17e-2) -	3.8222e-1 (1.45e-2) -	1.6967e-1 (3.77e-3)
		5000	1.7084e-1 (4.45e-3) ≈	6.0281e-1 (2.08e-2) -	3.8048e-1 (8.13e-3) -	1.6780e-1 (3.92e-3)
WFG8	2	1000	2.7310e-2 (6.87e-3) ≈	3.5654e-1 (6.06e-3) -	3.0381e-1 (1.12e-2) -	1.9648e-2 (2.87e-3)
		2000	2.5999e-2 (4.18e-3) ≈	3.6192e-1 (2.39e-2) -	2.9883e-1 (2.36e-2) -	1.6883e-2 (5.02e-3)
		5000	1.9362e-2 (2.02e-3) ≈	3.4778e-1 (1.64e-2) -	2.8571e-1 (2.59e-2) -	1.1687e-2 (9.90e-4)
	3	1000	3.0045e-1 (1.32e-2) -	4.5466e-1 (6.65e-3) -	3.8407e-1 (6.93e-3) -	1.6243e-1 (1.32e-2)
		2000	3.0091e-1 (5.79e-2) -	4.5961e-1 (2.32e-2) -	3.7365e-1 (2.12e-2) -	1.6056e-1 (1.62e-2)
		5000	2.0951e-1 (2.63e-2) -	4.6231e-1 (1.29e-2) -	3.5738e-1 (2.35e-2) -	1.6043e-1 (3.20e-2)
WFG9	2	1000	1.0775e-2 (3.40e-4) ≈	5.1925e-2 (6.05e-3) -	1.0343e-2 (2.39e-4) ≈	1.0967e-2 (2.42e-3)
		2000	1.1380e-2 (9.89e-4) -	4.5024e-2 (3.13e-3) -	1.0006e-2 (5.55e-4) -	9.1696e-3 (1.78e-4)
		5000	2.7806e-3 (6.37e-2) -	4.0592e-2 (2.12e-3) -	5.0613e-2 (4.78e-2) -	8.8244e-3 (5.90e-5)
	3	1000	1.7642e-1 (8.88e-3) -	2.0578e-1 (5.63e-3) -	1.6030e-1 (5.16e-4) ≈	1.6024e-1 (3.33e-4)
		2000	1.6765e-1 (6.22e-3) -	1.9641e-1 (8.38e-3) -	1.6034e-1 (4.02e-4) ≈	1.6018e-1 (3.02e-4)
		5000	1.6666e-1 (5.33e-3) -	1.9623e-1 (6.96e-3) -	1.6053e-1 (9.59e-4) ≈	1.5986e-1 (5.84e-4)
+/ - / ≈		15/18/21	6/48/0	0/45/9	-	

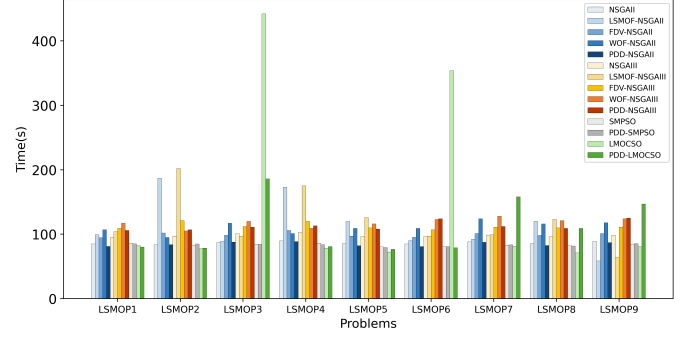
TABLE VII
STATISTICS OF IGD RESULTS OBTAINED BY FOUR COMPARED ALGORITHMS ON 15 TEST INSTANCES FROM ZDT TEST SUITE. THE BEST RESULT IS SHOWN IN BOLD FONT.

Problem	D	LMOEA-DS	CCGDE3	S ³ -CMA-ES	PDD-LMOCSO
ZDT1	1000	3.5395e-3 (2.40e-4) -	1.2901e+0 (3.17e-2) -	3.6463e+0 (5.35e-1) -	2.5838e-3 (1.89e-6)
	2000	3.4401e-3 (1.66e-4) -	1.4857e+0 (8.63e-2) -	3.5507e+0 (4.80e-1) -	2.5834e-3 (3.57e-6)
	5000	3.5454e-3 (1.14e-4) -	1.8987e+0 (1.20e-1) -	3.4376e+0 (4.51e-1) -	2.5879e-3 (5.02e-6)
ZDT2	1000	3.4633e-3 (2.22e-4) -	2.3090e+0 (9.40e-2) -	4.8173e+0 (8.16e-2) -	2.5296e-3 (1.12e-7)
	2000	3.4533e-3 (1.88e-4) -	2.5540e+0 (9.56e-2) -	4.8069e+0 (9.06e-2) -	2.5300e-3 (2.50e-7)
	5000	3.6806e-3 (1.48e-4) -	3.1491e+0 (9.46e-2) -	4.6789e+0 (5.00e-2) -	2.5308e-3 (1.95e-6)
ZDT3	1000	6.4815e-3 (5.19e-4) +	9.2485e-1 (1.32e-1) -	3.4140e+0 (5.90e-1) -	6.9621e-3 (1.47e-5)
	2000	6.3780e-3 (4.73e-4) +	1.1013e+0 (1.86e-1) -	3.6720e+0 (3.12e-1) -	6.9736e-3 (9.68e-6)
	5000	6.4486e-3 (2.98e-4) +	1.4244e+0 (2.25e-1) -	3.8068e+0 (2.90e-1) -	6.9569e-3 (1.76e-5)
ZDT4	1000	2.0451e+3 (2.48e+2) ≈	1.1912e+4 (1.91e+3) -	1.8282e+4 (2.79e+2) -	2.1240e+3 (1.95e+2)
	2000	7.2786e+3 (6.37e+2) -	2.5828e+4 (2.86e+3) -	3.6509e+4 (5.73e+2) -	5.2255e+3 (7.42e+2)
	5000	2.9790e+4 (8.05e+2) -	6.3869e+4 (6.89e+3) -	9.1508e+4 (4.05e+2) -	1.9284e+4 (4.13e+3)
ZDT6	1000	4.5639e-3 (3.08e-4) -	6.6581e+0 (5.94e-2) -	7.8823e+0 (3.15e-2) -	2.0617e-3 (8.96e-9)
	2000	4.9496e-3 (6.75e-4) -	6.9450e+0 (7.39e-2) -	7.9279e+0 (1.99e-2) -	2.0617e-3 (1.34e-8)
	5000	7.9996e-3 (4.64e-3) -	7.1986e+0 (1.03e-1) -	7.9223e+0 (1.84e-2) -	2.0617e-3 (1.16e-8)
+/ - / ≈		3/11/1	0/15/0	0/15/0	-

comparable to the comparison algorithms in the same group. Compared to state-of-the-art MOEAs for solving LSMOPs, our proposed PDD achieves outstanding performance without sacrificing computational efficiency. In contrast, although the LSMOF series have good performance in most problems, its calculation time is one order of magnitude higher than that of the comparison algorithms in the same group.

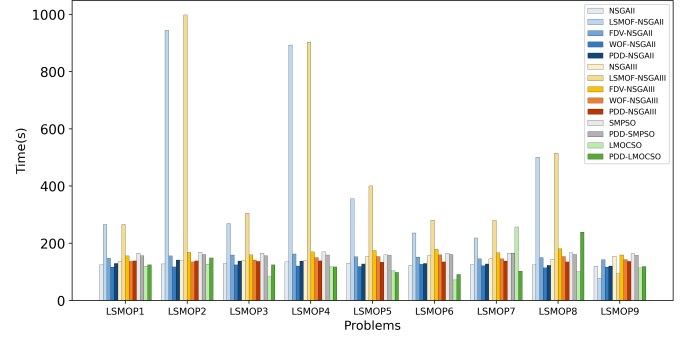
In summary, the proposed PDD shows superior performance with respect to solution quality and convergence speed when compared to existing frameworks of large-scale MOEAs. This effectively validates the efficacy and efficiency of the particle drift-diffusion process proposed for solving LSMOPs.

$M = 2, D = 1000$



(a)

$M = 3, D = 1000$



(b)

Fig. 8. Average computational time of 14 compared methods on bi-objective and tri-objective LSMOP1–LSMOP9 with 1000 decision variables. x-axis: test problems; y-axis: time(s). (a) $M = 2, D = 1000$. (b) $M = 3, D = 1000$.

F. PDD on the Application of Neural Network Training Problem

To further validate the effectiveness of PDD framework, we conduct a comparative experiment with real-world applications of neural network training problems. PDD embedded with MSKEA [46] (i.e., PDD-MSKEA) is compared with four other algorithms (LMOEA-DS, LMOCSO, DGEA and MSKEA). Neural network training problems can be regarded as multi-objective optimization problems, where the weights of feedforward neural networks are optimized by minimizing both model complexity and error rate [47], [48]. We select four different datasets (namely, Statlog_Australian, Climate, Statlog_German, and Connectionist_bench_Sonar) from the UCI machine learning repository [48]. The experiment had settings of $FE = 1 \times 10^4$ and $N = 150$.

Table X presents the HV results of the five algorithms on the selected datasets. It can be observed that PDD-MSKEA achieves three best results on four different training datasets, and its overall performance is significantly better than those of the comparison algorithms, i.e., LMOEA-DS, LMOCSO and DGEA. Compared to the original MSKEA, the overall performance of PDD embedded with MSKEA has been improved, which further proves the effectiveness of PDD in the application of LSMOPs.

TABLE VIII
STATISTICS OF IGD RESULTS OBTAINED BY PDD-NSGAI AND PDD-SMPSO WITH DIFFERENT SETTING OF RATE VALUES
($M = 2, D = 1000$).

Problem	PDD-NSGAI				PDD-SMPSO			
	Rate=0.2	Rate=0.4	Rate=0.6	Rate=0.8	Rate=0.2	Rate=0.4	Rate=0.6	Rate=0.8
LSMOP1	2.1788e-1 (5.50e-2)	1.9388e-1 (3.49e-2)	2.1700e-1 (3.22e-2)	2.4822e-1 (3.97e-2)	2.7853e-1 (1.91e-3)	2.8137e-1 (2.15e-3)	2.8301e-1 (3.04e-3)	2.8488e-1 (2.02e-3)
LSMOP2	1.5203e-2 (3.68e-4)	1.4967e-2 (7.06e-4)	1.4526e-2 (6.91e-4)	1.3701e-2 (6.13e-4)	7.6779e-3 (1.18e-4)	7.7251e-3 (1.70e-4)	7.6154e-3 (1.18e-4)	7.6090e-3 (1.27e-4)
LSMOP3	1.2018e+0 (2.48e-1)	1.1930e+0 (1.91e-1)	1.3108e+0 (2.21e-1)	1.3475e+0 (2.14e-1)	1.5663e+0 (1.07e-3)	1.5663e+0 (1.19e-3)	1.5667e+0 (7.45e-4)	1.5675e+0 (7.38e-4)
LSMOP4	3.3603e-2 (1.07e-3)	3.2467e-2 (1.40e-3)	3.1342e-2 (6.50e-4)	2.9711e-2 (1.02e-3)	2.1384e-2 (1.45e-4)	2.1428e-2 (1.84e-4)	2.1426e-2 (1.51e-4)	2.1386e-2 (1.16e-4)
LSMOP5	3.4727e-1 (1.39e-2)	3.4192e-1 (5.76e-3)	3.5081e-1 (3.64e-2)	3.3970e-1 (8.81e-3)	7.4209e-1 (1.15e-16)	7.4209e-1 (1.15e-16)	7.4209e-1 (1.15e-16)	7.4209e-1 (1.15e-16)
LSMOP6	3.8491e-1 (2.77e-2)	3.8251e-1 (3.48e-2)	3.7131e-1 (5.14e-2)	3.2757e-1 (7.80e-2)	1.7668e-1 (4.71e-3)	1.7673e-1 (5.40e-3)	1.7584e-1 (9.60e-3)	1.7547e-1 (6.57e-3)
LSMOP7	1.5112e+0 (9.57e-4)	1.5111e+0 (1.02e-3)	1.5114e+0 (1.04e-3)	1.5121e+0 (1.09e-3)	1.5110e+0 (5.51e-4)	1.5111e+0 (4.06e-4)	1.5111e+0 (3.62e-4)	1.5110e+0 (5.60e-4)
LSMOP8	3.5631e-1 (2.03e-2)	3.5611e-1 (2.87e-2)	3.6743e-1 (4.14e-2)	3.5953e-1 (3.42e-2)	4.8788e-1 (1.54e-2)	5.2678e-1 (2.20e-2)	5.5084e-1 (2.10e-2)	5.8926e-1 (2.18e-2)
LSMOP9	8.2153e-2 (5.09e-3)	8.5652e-2 (8.15e-3)	8.2273e-2 (2.68e-3)	8.3898e-2 (4.42e-3)	3.2752e-2 (6.34e-4)	3.2903e-2 (6.60e-4)	3.2649e-2 (5.60e-4)	3.2954e-2 (5.42e-4)
Mean Rank	2.625	2.5417	2.4931	2.3403	2.3403	2.6111	2.4097	2.8264

TABLE IX
STATISTICS OF IGD RESULTS OBTAINED BY PDD-NSGAI AND PDD-SMPSO WITH DIFFERENT SETTING OF S VALUES
($M = 2, D = 1000$).

Problem	PDD-NSGAI				PDD-SMPSO			
	S=2	S=5	S=8	S=10	S=2	S=5	S=8	S=10
LSMOP1	2.2964e-1 (4.10e-2)	2.0883e-1 (2.54e-2)	2.1397e-1 (3.23e-2)	2.2102e-1 (3.34e-2)	2.7952e-1 (2.61e-3)	2.8310e-1 (2.84e-3)	2.8611e-1 (2.89e-3)	2.8677e-1 (2.24e-3)
LSMOP2	1.4372e-2 (6.41e-4)	1.4375e-2 (6.31e-4)	1.4377e-2 (5.28e-4)	1.4422e-2 (5.22e-4)	7.6429e-3 (1.26e-4)	7.6679e-3 (1.42e-4)	7.6576e-3 (1.58e-4)	7.5936e-3 (1.30e-4)
LSMOP3	1.2545e+0 (2.10e-1)	1.3219e+0 (1.77e-1)	1.3651e+0 (2.14e-1)	1.3170e+0 (2.02e-1)	1.5662e+0 (1.08e-3)	1.5669e+0 (5.81e-4)	1.5673e+0 (6.24e-4)	1.5680e+0 (7.44e-4)
LSMOP4	3.2365e-2 (7.97e-4)	3.1053e-2 (7.72e-4)	3.0789e-2 (5.11e-4)	3.0706e-2 (9.78e-4)	2.1311e-2 (1.68e-4)	2.1366e-2 (1.12e-4)	2.1329e-2 (1.57e-4)	2.1368e-2 (1.18e-4)
LSMOP5	3.4003e-1 (2.40e-3)	3.4400e-1 (1.05e-2)	3.4146e-1 (5.64e-3)	3.4066e-1 (6.59e-3)	7.4209e-1 (1.15e-16)	7.4209e-1 (1.15e-16)	7.4209e-1 (1.15e-16)	7.4209e-1 (1.15e-16)
LSMOP6	3.8409e-1 (2.46e-2)	3.8138e-1 (3.47e-2)	3.7548e-1 (4.17e-2)	3.5488e-1 (6.68e-2)	1.7511e-1 (4.12e-3)	1.7429e-1 (5.60e-3)	1.7404e-1 (5.46e-3)	1.7722e-1 (7.05e-3)
LSMOP7	1.5118e+0 (1.31e-3)	1.5119e+0 (8.49e-4)	1.5116e+0 (8.90e-4)	1.5116e+0 (7.81e-4)	1.5111e+0 (3.39e-4)	1.5107e+0 (4.59e-4)	1.5111e+0 (2.83e-4)	1.5111e+0 (3.28e-4)
LSMOP8	3.6174e-1 (4.32e-2)	3.5275e-1 (3.15e-2)	3.4707e-1 (8.73e-3)	3.4884e-1 (1.18e-2)	5.1440e-1 (1.37e-2)	5.4356e-1 (1.90e-2)	5.9050e-1 (1.96e-2)	6.2453e-1 (2.23e-2)
LSMOP9	8.4251e-2 (3.71e-3)	8.2472e-2 (4.34e-3)	8.1697e-2 (2.93e-3)	8.1608e-2 (4.26e-3)	3.2434e-2 (4.45e-4)	3.2768e-2 (6.14e-4)	3.3228e-2 (6.61e-4)	3.3149e-2 (6.09e-4)
Mean Rank	2.6944	2.5208	2.4097	2.375	2.0347	2.2431	2.7083	3.0139

TABLE X
HV VALUES OF LMOEA-DS, LMOCSO, DGEA, MSKEA AND PDD-MSKEAR ON FOUR DATASETS FOR NEURAL NETWORK TRAINING.

Problem	D	Samples	Features	LMOEA-DS	LMOCSO	DGEA	MSKEA	PDD-MSKEAR
Statlog_Australian	321	690	14	3.5218e-1 (1.69e-2) -	3.4894e-1 (1.78e-2) -	3.4894e-1 (1.78e-2) -	8.8840e-1 (1.98e-3) +	8.8630e-1 (1.35e-3)
Climate	401	540	18	3.6854e-1 (1.99e-2) -	3.6536e-1 (1.88e-2) -	3.6536e-1 (1.88e-2) -	9.6429e-1 (5.27e-3) ≈	9.6620e-1 (4.34e-3)
Statlog_German	521	1000	24	3.1255e-1 (1.24e-2) -	3.1288e-1 (1.49e-2) -	3.1288e-1 (1.49e-2) -	8.0157e-1 (3.52e-3) ≈	8.0240e-1 (2.88e-3)
Connectionist_bench_Sonar	1241	208	60	3.2282e-1 (1.17e-2) -	3.2994e-1 (1.60e-2) -	3.2994e-1 (1.60e-2) -	8.1832e-1 (1.59e-2) -	8.3904e-1 (2.02e-2)
				+/- / ≈	0/4/0	0/4/0	0/4/0	1/1/2

V. CONCLUSION AND FUTURE WORK

In this study, we propose a novel framework called PDD for solving LSMOPs. The PDD framework simulates the motion patterns of particles in the physical world to identify effective solutions during the evolutionary process. The main contributions of PDD include the following aspects: 1) A guiding particle selection strategy is proposed to identify a subset of high-quality particles from the population. 2) A sub-stage division method is proposed to partition the evolutionary process into three sub-stages: two coarse-tuning sub-stages and a fine-tuning sub-stage. 3) A particle drift-diffusion process is proposed, wherein both drift and diffusion operations are applied during the coarse-tuning sub-stages to effectively simulate particle motion patterns. 4) A gradual shrinking diffusion operator is put forward, which progressively reduces the diffusion range of particles as the optimization process advances.

Comparative experiments were conducted in order to evaluate the effectiveness and efficiency of our proposed framework. The experimental results demonstrate that the particle drift-diffusion process in the PDD framework helps to maintain the diversity while improving the search efficiency, and our proposed framework outperforms many state-of-the-art frameworks, such as FDV, WOF and LSMOF, in terms of diversity and convergence. Therefore, our PDD framework can be considered an effective framework for solving LSMOPs.

Although the PDD framework shows promising potential in solving LSMOPs, it should be pointed out that optimal

parameter settings may vary for different problems. Future research will focus on developing automatic parameter tuning methods to adapt the framework to diverse problem instances.

REFERENCES

- [1] Li, B, Li, J, Tang, K and Yao, "Many-objective evolutionary algorithms: A survey," ACM Computing Surveys, vol. 48, no. 1, Sept. 2015.
- [2] M. Helbig and A. P. Engelbrecht, "Benchmarks for dynamic multi-objective optimisation," in Proceedings of the IEEE Symposium on Computational Intelligence in Dynamic and Uncertain Environments, pp. 84-91, Apr. 2013.
- [3] Z. Fan, Yi Fang, W. Li, Jiewei Lu, X. Cai and Caimin Wei, "A comparative study of constrained multi-objective evolutionary algorithms on Constrained Multi-Objective Optimization Problems," in Proceedings of the IEEE Congress on Evolutionary Computation, pp. 209-216, Jun. 2017.
- [4] Chugh, T., Sindhya, K., Hakanen, J. et al, "A survey on handling computationally expensive multiobjective optimization problems with evolutionary algorithms," Soft Computing, vol.23, pp. 3137-3166, May 2019.
- [5] K. Deb, A. Pratap, S. Agarwal, and T. Meyarivan, "A fast and elitist multiobjective genetic algorithm: NSGA-II," IEEE Transactions on Evolutionary Computation, vol. 6, no. 2, pp. 182-197, 2002.
- [6] K. Deb and H. Jain, "An evolutionary many-objective optimization algorithm using reference-point-based nondominated sorting approach, part I: Solving problems with box constraints," IEEE Transactions on Evolutionary Computation, vol. 18, no. 4, pp. 577-601, Aug. 2014.
- [7] Q. Zhang and H. Li, "MOEA/D: A multiobjective evolutionary algorithm based on decomposition," IEEE Transactions on Evolutionary Computation, vol. 11, no. 6, pp. 712-731, Dec. 2007.
- [8] K. Li, R. Chen, G. Fu and X. Yao, "Two-archive evolutionary algorithm for constrained multiobjective optimization," IEEE Transactions on Evolutionary Computation, vol. 23, no. 2, pp. 303-315, Apr. 2019.

- [9] Qing Cai, Lijia Ma, Maoguo Gong, and Dayong Tian, "A survey on network community detection based on evolutionary computation," *International Journal of Bio-Inspired Computation*, vol. 8, no. 2, pp. 84–98, 2016.
- [10] Jose Caceres-Cruz, Pol Arias, Daniel Guimaran, Daniel Riera and Angel A. Juan, "Rich vehicle routing problem: Survey," *ACM Computing Surveys*, vol. 47, pp. 1-28, 2014.
- [11] Jundong Li, Kewei Cheng, Suhang Wang, Fred Morstatter, Robert P. Trevino, Jiliang Tang and Huan Liu, "Feature selection: A data perspective," *ACM Computing Surveys*, vol. 50, pp. 1-45, 2017.
- [12] H. Li, Q. Zhang, J. Deng and Z. B. Xu, "A preference-based multiobjective evolutionary approach for sparse optimization," *IEEE Transactions on Neural Networks and Learning Systems*, vol. 29, no. 5, pp. 1716-1731, May 2018.
- [13] L. M. Antonio and C. A. Coello Coello, "Use of cooperative coevolution for solving large scale multiobjective optimization problems," in *Proceedings of the IEEE Congress on Evolutionary Computation*, pp. 2758–2765, Jun. 2013.
- [14] Miguel Antonio, L., Coello Coello, C.A., "Decomposition-based approach for solving large scale multi-objective problems," in *Proceedings of the International Conference on Parallel Problem Solving from Nature*, Springer, pp. 525–534, Aug. 2016.
- [15] A. Song, Q. Yang, W. N. Chen and J. Zhang, "A random-based dynamic grouping strategy for large scale multi-objective optimization," in *Proceedings of the IEEE Congress on Evolutionary Computation*, pp. 468-475, Jul. 2016.
- [16] Minghan Li and Jingxuan Wei, "A cooperative co-evolutionary algorithm for large-scale multi-objective optimization problems," in *Proceedings of the Annual Conference on Genetic and Evolutionary Computation Conference Companion*, pp. 1716-1721, Jul. 2018.
- [17] Frederick Sander, Heiner Zille, and Sanaz Mostaghim, "Transfer strategies from single- to multi-objective grouping mechanisms," in *Proceedings of the Genetic and Evolutionary Computation Conference*, pp. 729-736, Jul. 2018.
- [18] X. Ma, F. Liu, Y. Qi, X. Wang, L. Li, L. Jiao, M. Yin, M. Gong, "A multiobjective evolutionary algorithm based on decision variable analyses for multiobjective optimization problems with large-scale variables," *IEEE Transactions on Evolutionary Computation*, vol. 20, no. 2, pp. 275–298, Apr. 2016.
- [19] B. Cao, J. Zhao, Z. Lv and X. Liu, "A distributed parallel cooperative coevolutionary multiobjective evolutionary algorithm for large-scale optimization," *IEEE Transactions on Industrial Informatics*, vol. 13, no. 4, pp. 2030-2038, Aug. 2017.
- [20] X. Zhang, Y. Tian, R. Cheng, and Y. Jin, "A decision variable clustering-based evolutionary algorithm for large-scale many-objective optimization," *IEEE Transactions on Evolutionary Computation*, vol. 22, no. 1, pp. 97–112, Feb. 2018.
- [21] W. Du, W. Zhong, Y. Tang, W. Du and Y. Jin, "High-dimensional robust multi-objective optimization for order scheduling: A decision variable classification approach," *IEEE Transactions on Industrial Informatics*, vol. 15, no. 1, pp. 293-304, Jan. 2019.
- [22] Y. Tian, X. Zheng, X. Zhang, and Y. Jin, "Efficient large-scale multi-objective optimization based on a competitive swarm optimizer," *IEEE Transactions on Cybernetics*, vol. 50, no. 8, pp. 3696–3708, Aug. 2020.
- [23] Y. Tian, X. Zhang, C. Wang, and Y. Jin, "An evolutionary algorithm for large-scale sparse multiobjective optimization problems," *IEEE Transactions on Evolutionary Computation*, vol. 24, no. 2, pp. 380–393, Apr. 2020.
- [24] C. He, R. Cheng, and D. Yazdani, "Adaptive offspring generation for evolutionary large-scale multiobjective optimization," *IEEE Transactions on Systems, Man, and Cybernetics: Systems*, vol. 52, no. 2, pp. 786-798, Feb. 2022.
- [25] R. Cheng, Y. Jin, K. Narukawa and B. Sendhoff, "A Multiobjective Evolutionary Algorithm Using Gaussian Process-Based Inverse Modeling," *IEEE Transactions on Evolutionary Computation*, vol. 19, no. 6, pp. 838-856, Dec. 2015.
- [26] Huangke Chen, Ran Cheng, Jinming Wen, Haifeng Li, Jian Weng, "Solving large-scale many-objective optimization problems by covariance matrix adaptation evolution strategy with scalable small subpopulations," *Information Sciences: an International Journal*, vol. 509, pp. 457-469, Jan. 2020.
- [27] C. He, S. Huang, R. Cheng, K. C. Tan and Y. Jin, "Evolutionary multiobjective optimization driven by generative adversarial networks (GANs)," *IEEE Transactions on Cybernetics*, vol. 51, no. 6, pp. 3129-3142, June 2021.
- [28] H. Zille, H. Ishibuchi, S. Mostaghim, and Y. Nojima, "A framework for large-scale multiobjective optimization based on problem transformation," *IEEE Transactions on Evolutionary Computation*, vol. 22, no. 2, pp. 260–275, Apr. 2018.
- [29] C. He, L. Li, Y. Tian, X. Zhang, R. Cheng, Y. Jin, X. Yao, "Accelerating large-scale multiobjective optimization via problem reformulation," *IEEE Transactions on Evolutionary Computation*, vol. 23, no. 6, pp. 949–961, Dec. 2019.
- [30] S. Qin, C. Sun, Y. Jin, Y. Tan and J. Fieldsend, "Large-scale evolutionary multiobjective optimization assisted by directed sampling," *IEEE Transactions on Evolutionary Computation*, vol. 25, no. 4, pp. 724-738, Aug. 2021.
- [31] Y. Feng, L. Feng, S. Kwong and K. C. Tan, "A multivariation multifactorial evolutionary algorithm for large-scale multiobjective optimization," *IEEE Transactions on Evolutionary Computation*, vol. 26, no. 2, pp. 248-262, April 2022.
- [32] S. Liu, Q. Lin, L. Feng, K. C. Wong and K. C. Tan, "Evolutionary multitasking for large-scale multiobjective optimization," *IEEE Transactions on Evolutionary Computation*, vol. 27, no. 4, pp. 863-877, Aug. 2023.
- [33] X. Yang, J. Zou, S. Yang, J. Zheng and Y. Liu, "A fuzzy decision variables framework for large-scale multiobjective optimization," *IEEE Transactions on Evolutionary Computation*, vol. 27, no. 3, pp. 445-459, June 2023.
- [34] S. Wang, J. Zheng, Y. Liu, J. Zou, S. X. Yang, "An extended fuzzy decision variables framework for solving large-scale multiobjective optimization problems," *Information Sciences*, Vol. 643, Sep. 2023.
- [35] I. Giagkiozis, R. C. Purshouse, and P. J. Fleming, "An overview of population-based algorithms for multi-objective optimisation," *International Journal of Systems Science*, vol. 46, no. 9, pp. 1572–1599, 2015.
- [36] R. Cheng, Y. Jin, M. Olhofer and B. Sendhoff, "Test problems for large-scale multiobjective and many-objective optimization," *IEEE Transactions on Cybernetics*, vol. 47, no. 12, pp. 4108-4121, Dec. 2017.
- [37] S. Huband, P. Hingston, L. Barone, and L. While, "A review of multiobjective test problems and a scalable test problem toolkit," *IEEE Transactions on Evolutionary Computation*, vol. 10, no. 5, pp. 477–506, Oct. 2006.
- [38] E. Zitzler, K. Deb, and L. Thiele, "Comparison of multiobjective evolutionary algorithms: Empirical results," *Evolutionary Computation*, vol. 8, no. 2, pp. 173–195, 2000.
- [39] A. J. Nebro, J. J. Durillo, J. Garcia-Nieto, C. A. Coello Coello, F. Luna and E. Alba, "SMPSO: A new PSO-based metaheuristic for multi-objective optimization," in *Proceedings of the IEEE Symposium on Computational Intelligence in Multi-Criteria Decision-Making*, pp. 66-73, 2009.
- [40] S. Liu, J. Li, Q. Lin, Y. Tian and K. C. Tan, "Learning to accelerate evolutionary search for large-scale multiobjective optimization," *IEEE Transactions on Evolutionary Computation*, vol. 27, no. 1, pp. 67–81, Feb. 2023.
- [41] Y. Tian, R. Cheng, X. Zhang, and Y. Jin, "PlatEMO: A MATLAB platform for evolutionary multi-objective optimization [educational forum]," *IEEE Computational Intelligence Magazine*, vol. 12, no. 4, pp. 73–87, Nov. 2017.
- [42] P. A. N. Bosman and D. Thierens, "The balance between proximity and diversity in multiobjective evolutionary algorithms," *IEEE Transactions on Evolutionary Computation*, vol. 7, no. 2, pp. 174–188, Apr. 2003.
- [43] A. Zhou, Y. Jin, Q. Zhang, B. Sendhoff, and E. Tsang, "Combining model-based and genetics-based offspring generation for multi-objective optimization using a convergence criterion," *Proceedings of the IEEE International Conference on Evolutionary Computation*, pp. 892–899, Jul. 2006.
- [44] E. Zitzler, L. Thiele, M. Laumanns, C. M. Fonseca, and V. G. Da Fonseca, "Performance assessment of multiobjective optimizers: An analysis and review," *IEEE Transactions on Evolutionary Computation*, vol. 7, no. 2, pp. 117–132, Apr. 2003.
- [45] W. Haynes, "Wilcoxon rank sum test," *Encyclopedia of Systems Biology*, pp. 2354–2355, 2013.
- [46] Z. Ding, L. Chen, D. Sun, and X. Zhang, "A multi-stage knowledge-guided evolutionary algorithm for large-scale sparse multi-objective optimization problems," *Swarm and Evolutionary Computation*, vol. 73, pp.101-119, Aug. 2022.
- [47] Y. Tian, C. Lu, X. Zhang, K. C. Tan and Y. Jin, "Solving large-scale multiobjective optimization problems with sparse optimal solutions via unsupervised neural networks," *IEEE Transactions on Cybernetics*, vol. 51, no. 6, pp. 3115-3128, June 2021.
- [48] D. Dheeru and E. K. Taniskidou, "UCI machine learning repository," 2017. [Online]. Available: <http://archive.ics.uci.edu/ml>